CADMIUM ISOTOPIC COMPOSITION IN THE OCEAN

LACAN Francois[a*], FRANCOIS Roger[a†], JI Yongcheng[b] and SHERRELL Robert M.[b].

(a) Woods Hole Oceanographic Institution, Department of Marine chemistry and Geochemistry, Woods Hole, MA 02543, USA.

(b) Institute of Marine and Coastal Sciences and Department of Geological Sciences, Rutgers University, 71 Dudley Road, New Brunswick, NJ 08901-8521, USA.

* Corresponding author, now at

CNRS, LEGOS, UMR5566, CNRS-CNES-IRD-UPS, Observatoire Midi-Pyrenees, 18, Av. E. Belin, 31400 Toulouse, France

francois.lacan@legos.cnes.fr Phone: +33. 5.61.33.30.43 Fax: +33. 5.61.25.32.05

† now at Department of Earth and Ocean Sciences, The University of British Columbia, 6339 Stores Road, Vancouver, British Columbia, Canada, V6T 1Z4.

- Manuscript submitted to Geochimica et Cosmochimica Acta, December 20, 2005.

4 tables, 11 figures.

- Revised, June, 29, 2006

ABSTRACT

The oceanic cycle of cadmium is still poorly understood, despite its importance for phytoplankton growth and paleoceanographic applications. As for other elements that are biologically recycled, variations in isotopic composition may bring unique insights. This article presents i) a protocol for the measurement of cadmium isotopic composition (Cd IC) in seawater and in phytoplankton cells; ii) the first Cd IC data in seawater, from two full depth stations, in the northwest Pacific and the northwest Mediterranean Sea; iii) the first Cd IC data in phytoplankton cells, cultured in vitro. The Cd IC variation range in seawater found at these stations is not greater than 1.5 $\varepsilon_{Cd/amu}$ units, only slightly larger than the mean uncertainty of measurement (0.8 $\varepsilon_{Cd/amu}$). Nevertheless, systematic variations of the Cd IC and concentration in the upper 300m of the northwest Pacific suggest the occurrence of Cd isotopic fractionation by phytoplankton uptake, with a fractionation factor of 1.6±1.4 $\varepsilon_{Cd/amu}$ units. This result is supported by the culture experiment data suggesting that freshwater phytoplankton (*Chlamydomonas reinhardtii* and *Chlorella sp.*) preferentially take up light Cd isotopes, with a fractionation factor of 3.4±1.4 $\varepsilon_{Cd/amu}$ units. Systematic variations of the Cd IC and hydrographic data between 300 and 700m in the northwest Pacific have been tentatively attributed to the mixing of the mesothermal (temperature maximum) water ($\varepsilon_{Cd/amu}$=-0.9±0.8) with the North Pacific Intermediate Water ($\varepsilon_{Cd/amu}$=0.5±0.8). In contrast, no significant Cd IC variation is found in the northwest Mediterranean Sea. This observation was attributed to the small surface Cd depletion by phytoplankton uptake and the similar Cd IC of the different water masses found at this site.

Overall, these data suggest that i) phytoplankton uptake fractionates Cd isotopic composition to a measurable degree (fractionation factors of 1.6 and 3.4 $\varepsilon_{Cd/amu}$ units, for the in situ and culture experiment data, respectively), ii) an open ocean profile of Cd IC shows upper water column variations consistent with preferential uptake and regeneration of light Cd isotopes, and iii) different water masses may have different Cd IC. This isotopic system could therefore provide information on phytoplankton Cd uptake and on water mass trajectories and mixing in some areas of the ocean. However, the very small Cd IC variations found in this study indicate that applications of Cd isotopic composition to reveal aspects of the present or past Cd oceanic cycle will be very challenging and may require further analytical

improvements. Better precision could possibly be obtained with larger seawater samples, a better chemical separation of tin and a more accurate mass bias correction through the use of the double spiking technique.

1. INTRODUCTION

Although cadmium can be a toxic element at high concentrations, it is taken up by phytoplankton at the lower concentrations found in ocean surface waters, and may play a role in phytoplankton nutrition. The vertical oceanic distribution of dissolved Cd is typical of that of a nutrient, with a surface depletion, a maximum associated with organic matter remineralization and relatively constant values at depth. Dissolved Cd distribution in the ocean is closely correlated to that of phosphate (Boyle et al., 1976; Bruland et al., 1978).

The Cd/Ca ratio recorded in foraminiferal tests has been exploited to reconstruct past oceanic PO_4 distributions and infer past oceanic circulation and nutrient concentrations during the last glacial maximum, in the context of long-term climate variations (Boyle, 1988; Elderfield and Rickaby, 2000). However, although the Cd versus P relationship is very consistent in deep waters, substantial deviations have been documented in surface waters, in particular in High Nutrient Low Chlorophyll (HNLC) areas of the Subarctic Pacific (e.g. Martin et al., 1989) and Southern Oceans (e.g. Frew and Hunter, 1992). Although these deviations can be accounted for by empirical models based on the modern Cd and P distributions (e.g. Elderfield and Rickaby, 2000; Sunda and Huntsman, 2000), the mechanisms yielding these deviations have only begun to be explored (Cullen et al., 2003; Cullen, 2006).

It has been shown that Cd can substitute for Zn in Zn-carbonic-anhydrase (an enzyme involved in inorganic carbon acquisition; (Price and Morel, 1990; Morel et al., 1994) or used directly in a Cd-specific form of the enzyme (Cullen et al., 1999; Lane et al., 2005). However the factors controlling Cd concentration is seawater are still poorly understood. Zinc concentration (Price and Morel, 1990), CO_2 partial pressure (Cullen et al., 1999), growth rate and Fe or Mn availability (Sunda and Huntsman, 2000; Frew et al., 2001; Cullen et al., 2003) are all factors that could substantially influence Cd uptake by phytoplankton.

These recent findings underscore the need for a better understanding of the oceanic cadmium cycle. Owing to the large mass range of the Cd isotopic system (from ^{106}Cd to ^{116}Cd), biological uptake, adsorptive scavenging and remineralization of organic matter could produce Cd isotopic fractionations.

Cadmium isotopic data may therefore provide new insight into these processes. In particular, biologically mediated Cd isotopic fractionation could be significant. In such a case, for areas in which surface water Cd depletion is partial (as in N-limited or HNLC areas, where excess phosphate is found), the Cd isotopic composition (Cd IC) of surface waters and in turn that of the exported organic matter could vary according to Rayleigh fractionation. Cd isotopic measurements in seawater or exported organic matter could therefore allow quantification of the degree extent of Cd utilization. If significant Cd isotopic fractionations occur in the environment, this parameter could also help to trace different Cd sources and transports in the ocean.

As a first step towards elucidating the systematics of Cd isotopic fractionation in the environment, we present the first cadmium isotope measurements in seawater (northwest Pacific and northwest Mediterranean), and in phytoplankton (cultured freshwater green algae, C*hlamydomonas reinhardtii sp.* and *Chlorella sp.*).

2. SAMPLES

The seawater samples were taken from the northwest Pacific (Cruise MR02-K05 Leg2, 16/10/2002, Station K1, 51.28°N, 165.2°E, 5140 m depth) and at the DYFAMED site in the Mediterranean Sea (Cruise Barmed 5, 25/06/2003, 43.4°N, 7.9°E, 2350 m depth) (Fig. 1). These two sites represent very different oceanic regimes with distinct Cd and nutrient distributions. Cadmium and P concentrations are approximately an order of magnitude higher at station K1 than at DYFAMED (Fig. 2). There is near complete surface phosphate depletion at DYFAMED, which is not the case at K1. The Cd cycle in the Mediterranean is unique. Surface Cd concentrations are much higher than in nutrient-depleted waters of the open ocean (Boyle et al., 1985; van Geen et al., 1991). This enrichment could have various natural or anthropogenic origins, such as advection with river waters, aeolian inputs or shelf sediment remobilization (Riso et al., 2004 and references therein).

Depending on the sampling site, 250 (North Pacific) to 1000 mL (Mediterranean) of unfiltered seawater were acidified with trace metal clean HCl to pH<2. Subsequent sample handling was conducted

under stringent trace metal clean conditions. Whereas it is commonly accepted that particulate Cd is a negligible fraction of dissolved at depth, this is not necessarily the case for surface waters. There are few studies reporting both dissolved and particulate Cd concentration in seawater. In the Atlantic Ocean surface water (40°N to 20°S), particulate Cd concentrations amount to ~ 3.3% of total Cd (values ranging from 0.7 to 9%. Helmers, 1996). In the northeast Pacific, Sherrell (1989) reports particulate Cd concentration decreasing from about 4 pmol L^{-1} at 30m to 0.10 to 0.15 pmol L^{-1} at 2000-3000m, whereas surface dissolved Cd content in this area were found around 60 pmol L^{-1} (Bruland, 1980). Taken together, these two studies suggest that particulate Cd amounts to ~ 6% of total Cd in the surface waters of the northeast Pacific and to much less at depth. Finally, dissolved Cd data from the surface waters of the northwest Pacific are identical to our total Cd data (when comparing samples at similar depths and similar hydrographical properties. Abe, 2002), suggesting negligible particulate Cd content at this site. We therefore assume that the Cd concentrations and isotopic compositions measured in this study characterize primarily dissolved Cd.

Two species of freshwater phytoplankton were selected in this study: *Chlamydomonas reinhardtii sp.* and *Chlorella sp*. The algae were grown in vitro (Institute of Marine and Coastal Sciences, Rutgers University) in acid-washed 1L polycarbonate bottles under 100 μmol quanta $m^{-2}s^{-1}$ light illumination with 12:12h light:dark cycle at 19±1 °C. Bacterial biomass was controlled to negligible levels by microwave heating of the media to near 100°C prior to phytoplankton inoculation. Replicate culture bottles (4 per species) were grown in low-metal nutrient replete freshwater media (pH ~7.0), in which the trace metals were buffered by 5μM EDTA. The total metal concentration in the culture media was: Fe: 116nM; Mn: 13nM; Zn: 27.2nM; Cu: 44.3nM; Co: 4nM; Cd: 17.3nM, and Ni: 3520nM. Buffered by 5μM EDTA, these total metal concentrations correspond to equilibrium Me' (the concentration of free metal ions plus labile dissolved inorganic species) of: Fe, 40pM; Mn, 2nM; Zn, 20pM; Cu, 0.14 pM; Co, 2pM; Cd, 7.9pM and Ni, 20pM (calculated using the chemical speciation program MINEQL+, version 5.0). Cadmium was added to the concentrated mixed metal stock solution as $CdCl_2$ (Aldrich Chem Co., >99.99%), and less than 1% of total Cd in the media was removed by phytoplankton uptake during the

incubation. Accordingly, we assume that the Cd isotopic composition of the media did not change during phytoplankton growth.

The phytoplankton were acclimated to the experimental media for several generations and inoculated into fresh media to initiate the incubation from which isotope fractionation was determined. Cells were harvested at mid-exponential growth stage (cell density ~ 200,000 cells mL^{-1}) by centrifugation at 6500 rpm (3000xg) (Eppendorf model 5403) using six 50mL polycarbonate centrifuge tubes for 15 min at 19°C. After centrifugation, cell pellets were rinsed twice with 50mL Milli-Q deionized H_2O to wash away any residual media (>99.99% removal), thus eliminating the contribution of metals from residual media to the cell pellet. Each sample represents combined cell pellets from 2 culture bottles. The pooled pellets were concentrated to a <0.5mL suspension, which was transferred into 15mL screw-cap Teflon vials for digestion in 1mL 16N trace metal clean HNO_3 (Baseline, SeaStar Chemical) at 120°C for four hours on a hotplate. Digest solutions were then dried on a hotplate (60°C) and redissolved in 1.2N HCl (Baseline, SeaStar Chemical). All handling steps were carried out in a HEPA Class 100 clean bench. Once in 1.2N HCl, the samples were processed and measured following the analytical protocol described below. In addition, samples of $CdCl_2$ powder, mixed-metal stock solution, and post-harvest media supernatant were retained for isotopic analysis to characterize thoroughly the isotopic composition of the source Cd.

3. ANALYTICAL PROCEDURES

The measurement of the Cd isotopic composition (Cd IC) in seawater and plankton cells requires its extraction from the sample matrix, with i) a high yield (because of its low abundance), ii) low contamination levels, iii) no isotopic fractionation and iv) a sufficient separation of the elements interfering with the Cd isotopes during the spectrometric analysis (mainly Pd, In and Sn, cf. Table 1 and section 3.2.1. for further details).

3.1 Chemical separation

Whereas Cd extraction from seawater requires a preconcentration procedure due to its low abundance, this step is useless for plankton samples. Seawater samples were therefore processed through a Chelex and AGMP1 resins, as described below, whereas plankton samples were processed through the AGMP1 resin only.

3.1.1. Transition metals separation from seawater matrix

This protocol is adapted from Kingston et al. (1978). The pH of the acidified seawater samples was raised to ~5.5 by adding concentrated NH_4OH and buffering with Maleic Acid/Ammonium Hydroxide (pH=5.8. Pai et al., 1990). Two mL of Biorad® Chelex 100 resin (in 2N HNO_3), 100-200 mesh, were packed in a Biorad® polyprep column (bed volume: 2 mL, conical, 0.8 cm mean internal diameter, 4 cm height; 10 mL reservoir). The resin was converted to its ammonia form with 6 mL of 2N NH_4OH and rinsed with 6 mL of MQ water. The samples were pumped through the resin with a peristaltic pump at a flow rate less than 1 mL min^{-1} (acid cleaned Tygon® tubing was used). The major seawater cations were eluted with 30 mL of 1N NH_4Ac at pH=5. After rinsing with 6 mL of MQ water, the transition metals were eluted with 9 mL 2N HNO_3. The eluates were then evaporated and redissolved in 1 mL 1.2N HCl for the next separation. The resin and tubing were cleaned with 20 mL 2N HNO_3 and rinsed for future use.

3.1.2. Cadmium separation

The following protocol is based on a personal communication by C. Cloquet (CRPG, Nancy, France). Two mL of Biorad® AGMP1 resin were packed in a Biorad® polyprep column. The resin was first cleaned following the sequence: 10 mL 6N HCl, 10 mL water, 10 mL 0.5N HNO_3, 10 mL water, 10

mL 8N HF + 2N HCl, 10 mL water, 10 mL 0.5N HNO3 and 10mL water. The resin was then conditioned with 10 mL 1.2N HCl and the sample loaded in 1 mL 1.2N HCl. The elution was done following the sequence: 4 mL 1.2N HCl (elution of the matrix), 15 mL 0.3N HCl (elution of Pb, Sn), 17mL 0.012N HCl (elution of Pb, Sn, Zn) and 16 mL 0.0012N HCl to elute the Cd. The Cd eluates were then evaporated and redissolved in 0.6 mL 0.5N HNO_3 for spectrometric analysis.

3.2. Spectrometric analysis

All results are reported as $\varepsilon^{i/j}_{Cd/amu}$ which is the deviation of the Cd isotope composition of a sample relative to a reference material in parts per 10 000, normalized to a mass difference of one atomic mass unit (amu):

$$\varepsilon^{i/j}_{Cd/amu} = \left(\frac{\left(\frac{^{i}Cd}{^{j}Cd} \right)_{Sample}}{\left(\frac{^{i}Cd}{^{j}Cd} \right)_{Reference}} - 1 \right) \times \frac{10000}{m_i - m_j} \qquad (1)$$

Where i and j refer to the isotopes of mass m_i and m_j. The "/amu" notation facilitates the comparison of data obtained from different isotope ratios. Increasing values of $\varepsilon^{i/j}_{Cd/amu}$ reflect enrichment in heavy Cd isotopes, whatever i and j values are used. Rigorously, such comparison should take into account the mass fractionation law that describes the isotope fractionation process. However, considering the range of variation of our dataset (<0.5‰ amu^{-1}), the discrepancies between this rigorous approach and the simple mass difference normalization used here are negligible (Wombacher and Rehkämper, 2004). The reference material used in this work is the JMC standard solution (Wombacher et al., 2003).

Cadmium isotopic ratios were measured on a ThermoFinnigan Neptune multiple collector inductively coupled plasma mass spectrometer (MC-ICPMS, WHOI). The instrument parameters are

summarized in Table 2. Samples were introduced with a desolvating nebulizer (CETAC Aridus System) to maximize the efficiency of sample introduction into the plasma and to reduce oxide formation and interferences.

Isotopic ratios measured with a MC-ICPMS must be corrected for i) a relatively large, but steady, instrumental mass fractionation, ii) spectral interferences and iii) matrix effects (discussed in section 3.3.).

3.2.1. Interference corrections

Tin (Sn), indium (In) and palladium (Pd) can produce isobaric interferences with Cd (Table 1). Therefore, the abundances of ^{117}Sn, ^{105}Pd and ^{115}In are measured in addition to Cd isotopes. The Faraday cup configuration is shown in Table 1. The method first measures the isotopic ratios of Cd and Ag (used for instrumental mass fractionation correction, see below) and ^{117}Sn. Subsequently, the magnetic field is shifted twice in order to successively and quickly measure ^{105}In and ^{115}Pd. In and Pd were always found at insignificant levels, so that these two steps were only systematic verifications of their non-occurrence. Significant levels of Sn were observed, however, which required correcting for this interference. Molecular interferences (eg. molybdenum oxides and zinc argides) were found to be insignificant (cf. section 3.3.).

Tin produces interferences on ^{112}Cd, ^{114}Cd and ^{116}Cd. To a first approximation, one could estimate the ^{112}Sn, ^{114}Sn and ^{116}Sn abundances from the measured ^{117}Sn peak intensity and the mean natural isotopic abundance for Sn. With MC-ICP-MS, however, instrumental fractionation of isotopes during measurements is substantial (up to 100's epsilon units) and much larger than the small natural fractionation that we are trying to measure (a few epsilon units). In order to estimate accurately the Sn isobaric interferences, we thus need to correct for Sn instrumental mass fractionation. Mass fractionation is traditionally modeled by linear, power or exponential laws (Russel et al., 1978). Marechal et al. (1999) suggested that the exponential law provide a more consistent correction than the linear and the power laws. Wombacher et al. (2003) also preferred the exponential law for describing Cd fractionation by MC-

ICPMS. We will show in section 3.2.2. that the exponential law was also the most suitable for Cd fractionation corrections. This law is therefore used here for Sn interference corrections.

Let $M_{^iX}$ and $M_{^jX}$ be the masses of ^iX and ^jX, two isotopes of the same element, with $\Delta M_{i,j_X} = M_{^jX} - M_{^iX}$. Let R_{i,j_X} and r_{i,j_X} be the true and instrumentally fractionated abundance ratios of isotope ^jX relative to isotope ^iX. In the absence of interferences, r_{i,j_X} is the parameter measured with the spectrometer: $r_{i,j_X} = I_{^jX} / I_{^iX}$, where I_α is the beam intensity produced by isotope α (note that in the presence of interferences, I_α is not directly measured and therefore neither is r_{i,j_X}). The exponential law postulates that the logarithmic fractionation $\ln\left(r_{i,j_X}/R_{i,j_X}\right)$ is, to the first order, proportional to the mass logarithm difference $\Delta \ln M_{i,j_X} = \ln M_{^jX} - \ln M_{^iX}$ (Marechal et al., 1999):

$$\ln\left(\frac{r_{i,j_X}}{R_{i,j_X}}\right) \approx f \times \Delta \ln M_{i,j_X} \qquad (2)$$

where f is the mass independent exponential law mass fractionation coefficient. Equation (2) is equivalent to:

$$r_{i,j_X} \approx R_{i,j_X}\left(\frac{M_{^jX}}{M_{^iX}}\right)^f \quad (3)$$

Given ^kX and ^lX two other isotopes of the same element, (2) implies:

$$\ln\left(r_{k,l_X}\right) \approx \frac{\Delta \ln M_{k,l_X}}{\Delta \ln M_{i,j_X}} \times \ln\left(r_{i,j_X}\right) - \frac{\Delta \ln M_{k,l_X}}{\Delta \ln M_{i,j_X}} \times \ln\left(R_{i,j_X}\right) + \ln\left(R_{k,l_X}\right) \qquad (4)$$

(4) is equivalent to:

$$R_{k,l_X} \approx r_{k,l_X} \times \left(\frac{R_{i,j_X}}{r_{i,j_X}}\right)^{\left(\ln\frac{M_{l_X}}{M_{k_X}} \Big/ \ln\frac{M_{j_X}}{M_{i_X}}\right)} \qquad (5)$$

If we were to measure the ratio of two Sn isotopes free of significant interferences (eg. ^{117}Sn and ^{118}Sn) and compare the results to an accepted "mean" natural abundance (Rosman and Taylor, 1998), the difference would mainly reflect the relatively larger instrumental fractionation, albeit with a small,

variable and unknown contribution from natural fractionation in the samples. Applying equation (2) using measured (r) and accepted (R) ratios would thus provide a good approximation for f:

$$f = \ln\left(\frac{r_{117,118\,Sn}}{R_{117,118\,Sn}}\right) \times \frac{1}{\ln(M_{118\,Sn}) - \ln(M_{117\,Sn})} \quad (6)$$

This value could then be used to estimate Sn contributions to the measured beam intensity for masses 112, 114 and 116, according to equation (3), eg. for ^{112}Sn :

$$I_{112\,Sn} = I_{117\,Sn} \times R_{117,112\,Sn} \times \left(\frac{M_{112\,Sn}}{M_{117\,Sn}}\right)^{f} \quad (7)$$

Note that $I_{112\,Sn}$ is defined as the beam intensity produced by ^{112}Sn, which is different from the beam intensity measured for mass 112, I_{112}, which includes contributions from different isotopes to the beam (here Sn and Cd). On the other hand, since no significant interference occurs for ^{117}Sn, $I_{117\,Sn}$ is equal to I_{117}.

These interferences ($I_{112\,Sn}$, $I_{114\,Sn}$, $I_{116\,Sn}$) could then be corrected, by subtracting the Sn contributions from the beam intensities measured for masses 112, 114 and 116 (which are the sum of Cd and Sn contributions), eg. for ^{112}Sn:

$$I_{112\,Cd} = I_{112} - I_{112\,Sn} \quad (8)$$

However, the collector configuration that we chose did not allow direct estimation of Sn mass fractionation, as doing so would have required longer analyses and therefore larger samples. Instead, we estimated f using two Cd isotopes free of isobaric interference (^{110}Cd and ^{111}Cd) and assumed that f calculated for Cd holds for Sn (as previously done by Wombacher et al. 2003). There is some level of circularity in this procedure, since our ultimate goal is to measure small natural variations in Cd isotopic composition and here we assume that there is no natural Cd isotopic fractionation. However, the latter (a few epsilon units) is approximately two orders of magnitude smaller than the instrumental fractionation

(up to 100's epsilons units). Therefore the error on the Sn mass fractionation estimation is only on the order of a few percent. Since ^{112}Sn and ^{114}Sn interferences were always lower than 1% and 0.5% of the Cd signals, respectively, the method yielded small errors on the interference corrections and provided meaningful Cd isotopic ratios (although, this procedure was less suitable for ^{116}Cd, due to the much larger ^{116}Sn contribution on mass 116). This was further verified by estimating f using two Ag isotopes (^{107}Ag and ^{109}Ag), which yielded similar results.

The validity of the Sn interference correction was assessed following the method proposed by Wombacher et al. (2003). Cadmium isotopic ratios corrected for Sn interferences were normalized using the exponential law to a "true" Cd ratio. Such normalization should (if Cd obeys this fractionation law) remove simultaneously the instrumental and natural fractionations. Thus, if the interferences were accurately corrected, all samples should display the same Cd isotopic ratios. Results of this test are shown in Fig. 3. Whereas the uncorrected $\varepsilon^{114/111}_{Cd/amu}$ data display significant anomalies (up to 3.7 units), the Sn interference corrected anomalies are restricted to the range [-0.3,+0.5]. In the case of ^{112}Cd, the Sn uncorrected $\varepsilon^{112/111}_{Cd/amu}$ display anomalies up to 19 units, which are restricted to the range [-0.5,+0.7] after correction. In the case of ^{116}Cd (results not shown for clarity purposes), the Sn uncorrected $\varepsilon^{116/111}_{Cd/amu}$ display anomalies up to 179 units, which are restricted to the range [-0.5,+0.9] after correction. These results show that Sn interference corrections are adequate (reducing the interferences by a factor larger than 300, in some cases). However, for isotopes with larger interferences (notably ^{116}Cd) Sn interference corrections can sometimes be too uncertain to produce useful Cd isotopic data.

3.2.2. Instrumental mass fractionation

After correcting for isobaric interferences, the Cd instrumental mass fractionation must be considered. Several methods are available to estimate instrumental mass fractionation. The standard bracketing method consists in bracketing each sample by reference standard measurements. The average

isotopic ratio from each two bracketing standard measurements is then taken as the reference ratio to calculate epsilon of the sample as per equation (1). However this method assumes a linear variation of the instrumental mass fractionation with time between standard measurements, which is not always the case, as shown by the sharp variation of the unnormalized data in Fig. 4.

A better approach consists in using the isotopic composition of a standard of a different element, in our case silver (Ag), added to the sample prior to the spectrometric analysis, to estimate instrumental mass fractionation. The main advantage of this method lies in the fact that the instrumental mass fractionation is monitored during the sample measurement. This method, called external (inter-element) normalization, assumes that the Cd and Ag isotope fractionations are related according to a known law. The exponential law, described above in the case of a single element, was shown to be appropriate for this purpose in several studies (e.g. Marechal et al., 1999; Wombacher et al., 2003). The correction was performed using equation 5, in which a pair of silver isotopes is substituted for a pair of Cd isotopes. The exponential normalization to Ag considerably reduced the dispersion of the standard $\varepsilon^{114/111}_{Cd/amu}$ values (which should all be equal to zero), the largest deviation from the mean being of 0.8 $\varepsilon_{Cd/amu}$ unit (Fig. 4). This results indicates that the logarithm of the measured ratio of two Cd isotopes ($\ln(r_{k,l\,Cd})$) must be a linear function of the logarithm of the measured ratio of two Ag isotopes ($\ln(r_{i,j\,Ag})$), with a proportionality factor equal to $\frac{\Delta \ln M_{k,l\,Cd}}{\Delta \ln M_{i,j\,Ag}}$ (equation 4). In other words, the data plotted in Fig. 5 should lie on a line with a slope of $\frac{\ln(M_{110Cd}/M_{114Cd})}{\ln(M_{107Ag}/M_{109Ag})} = 1.9292$. When looking at the whole dataset, this slope is found to be 1.9295±0.02 (1σ), in good agreement with the theoretical value. This agreement was found to be equally good for other Cd ratios (not shown here).

However, Fig. 5 also shows that the slope of the linear regression significantly varies between the different measurement sessions. Therefore, a variant of the exponential external normalization method, which uses the measured correlation between the Cd and Ag fractionation, can be used. This method, called the empirical normalization (described by Marechal et al., 1999), consists in using the slope

measured during a specific measurement session as shown in Fig. 5 instead of that predicted by the exponential law, following equation (9).

$$R_{k,l_{Cd}} \approx r_{k,l_{Cd}} \times \left(\frac{R_{i,j_{Ag}}}{r_{i,j_{Ag}}} \right)^{s} \quad (9)$$

Where s is the measured slope of the linear regression of $\ln\left(r_{k,l_{Cd}}\right)$ versus $\ln\left(r_{i,j_{Ag}}\right)$.

The results of the corrections obtained with the empirical method are shown in Fig. 4. The standard $\varepsilon^{114/111}_{Cd/amu}$ values are all very close to 0, the largest deviation from the mean being of 0.2 $\varepsilon_{Cd/amu}$ unit. These results are slightly better than those obtained with the exponential normalization. The empirical method was thus used to correct for instrumental fractionation in our samples.

For both the exponential and empirical method, the standard reference value used to calculate epsilon (Equation 1) can either be chosen as the average of the two standard measurements bracketing the sample, or as the average of the all standard measurements made within the measurement session. The latter option is used in this work, since it is more consistent with the normalization methods, which should theoretically lead to constant standard values; the variations observed reflecting the internal precision of the measurement.

3.3. Validation

3.3.1. Blanks

Total procedural blanks were estimated as follows: 250 mL of coastal seawater (Nantucket Sound, Mass. USA) were passed through three consecutive Chelex columns (following the procedure described above, section 3.1.1.). Assuming a repetitive yield of ~93% (see below), this procedure should have removed 99.97% of the Cd initially present. This “Cd-free” seawater was then analyzed following the

chemical procedure described above. This procedure simulates as accurately as possible the procedural blank, since the amount and matrix of the Cd-free samples used are similar to those of a real sample. The resulting Cd content was then measured by isotope dilution (by addition of a ^{108}Cd spike and measurement of the $^{108Cd}/^{111}$Cd ratio, free of Sn interference) and found to be 0.6 10^{-12} mol ± 4% (1σ). This represents less than 1% of our smallest sample and ~0.5% on average. This blank was therefore neglected.

3.3.2. Yields

The yield of the total procedure was estimated by subdividing a coastal seawater sample (Nantucket Sound, Mass. USA) into three pairs of samples of 250, 400 and 1000 mL. One sample of each pair was spiked with ^{108}Cd. The samples were then run through the entire column separation procedure. The unspiked samples were spiked after column separation. The Cd content of each sample was determined by isotope dilution, thereby providing the Cd concentration before and after the chemical procedure. The total yield was found to be ~86% ±1% and was independent of sample size. A similar technique was applied to the second AGMP1 column, only using a standard solution instead of a seawater sample to determine yield, found to be ~93%. The yield of the first Chelex column was thus estimated at ~93% (this yield could not be determined directly because the salt content of the Chelex column seawater eluate is still too high for direct ICPMS measurement).

3.3.3. Isotopic fractionation during column separation

Because the total yield of the chemical separation was lower than 100%, isotopic fractionation during column separation had to be assessed. This was done by addition of 10^{-7} g of the JMC Cd standard to 250 mL Cd-free seawater samples (prepared as described above), which were then analyzed following the normal procedure. The isotopic fractionation for the whole two-column method was found to be $\varepsilon_{\mathrm{Cd/amu}}^{110/114} = -0.2 \pm 0.2$. The isotopic fractionation of the second AGMP1 column alone was measured

separately by running a standard solution through the resin and was found to be $\varepsilon^{110/114}_{Cd/amu} = -0.3 \pm 0.2$. These results indicate that neither the Chelex nor the AGMP1 column fractionate significantly. The isotopic composition of the Cd-free seawater samples spiked with a realistic amount of Cd standard also shows that matrix effects are negligible.

3.3.4. Precision and accuracy

2.3.4.1. Internal precision. The internal precision (i.e. counting statistics) of the measurements, expressed as twice the standard error of the mean ($2\sigma_n$) were 0.4, 0.3 and 0.2 $\varepsilon_{Cd/amu}$ unit on average for the $^{110}Cd/^{111}Cd$, $^{112}Cd/^{111}Cd$ and $^{114}Cd/^{111}Cd$ ratios respectively (with maximum values of 0.9, 0.6 and 0.3 $\varepsilon_{Cd/amu}$ unit respectively, for the smallest sample).

3.3.4.2. External precision and reproducibility. The external precisions were estimated from the measurement of 30 JMC standard and found to be: 1.2 $\varepsilon_{Cd/amu}$ units (2σ) for the $^{110}Cd/^{111}Cd$ ratio by standard bracketing; 0.2, 0.1 and 0.4 $\varepsilon_{Cd/amu}$ unit (2σ) for the $^{110}Cd/^{111}Cd$, $^{112}Cd/^{111}Cd$ and $^{114}Cd/^{111}Cd$ ratios respectively by exponential normalization; 0.1, 0.1 and 0.2 $\varepsilon_{Cd/amu}$ unit (2σ) for the $^{110}Cd/^{111}Cd$, $^{112}Cd/^{111}Cd$ and $^{114}Cd/^{111}Cd$ ratios respectively by empirical normalization. These results confirm the good performances of the exponential and especially empirical normalizations. However, standard reproducibility does not account for variabilities due to matrix effects or interferences. Therefore, seven seawater duplicates from the North Pacific (Fig. 6a) were also measured and yielded a mean reproducibility of: 0.8 $\varepsilon_{Cd/amu}$ unit (empirical normalization), with a maximum discrepancy of 1.5 $\varepsilon_{Cd/amu}$ units (for $^{110}Cd/^{111}Cd$, $^{112}Cd/^{111}Cd$ and $^{114}Cd/^{111}Cd$ ratios). This reproducibility (0.8 $\varepsilon_{Cd/amu}$ unit) is the best assessment of the measurement precision, as it includes variations due to sample processing.

3.3.4.3. Accuracy. The fractionated "Münster" standard (Wombacher and Rehkämper, 2004), was measured three times and found to have an isotopic composition of $\varepsilon^{110/111}_{Cd/amu} = +11.1 \pm 0.5$ and

$\varepsilon^{114/111}_{Cd/amu} = +11.3 \pm 0.5$. These results are identical to the only other reported measurement (Wombacher and Rehkämper, 2004 ; measured by C. Cloquet in Nancy, +45 $\varepsilon^{114/110}$Cd.)

3.3.4.4. Inter-isotope consistency. In the case of the North Pacific station, different isotope ratios measured concurrently on seawater samples give results that are identical within measurement error (Fig. 7). The linear relationship between $\varepsilon^{110/111}_{Cd/amu}$ and $\varepsilon^{114/111}_{Cd/amu}$ (Fig. 7b) indicates that Cd isotope fractionation is mass dependant, which validates the analytical and measurement protocol. A similar linear relationship (although not as good, R^2=0.79, not shown here for clarity purposes) is found between $\varepsilon^{110/111}_{Cd/amu}$ and $\varepsilon^{112/111}_{Cd/amu}$, but not between $\varepsilon^{110/111}_{Cd/amu}$ and $\varepsilon^{116/111}_{Cd/amu}$. This shows that, in the case of the North Pacific samples, Sn interferences on ^{114}Cd and ^{112}Cd are satisfactorily corrected (with better corrections for ^{114}Cd) but interference on ^{116}Cd is not. These results validate the ^{110}Cd/^{111}Cd, ^{112}Cd/^{111}Cd and ^{114}Cd/^{111}Cd data, at the North Pacific station. The ^{114}Cd/^{111}Cd ratio is preferred to the ^{112}Cd/^{111}Cd ratio at this station, given the better interference correction on ^{114}Cd than on ^{112}Cd. Such a linear relationship is not found at the DYFAMED station (neither for ^{112}Cd, nor for ^{114}Cd, nor for ^{116}Cd). This suggests that Sn interferences are unsatisfactorily corrected for all Cd isotopes, which very likely results from the lower Cd content of these samples (6 to 8.5 ng, compared to 12 to 25 ng for the North Pacific samples), resulting in significantly higher Sn interferences at DYFAMED than at the North Pacific station. The ^{112}Cd, ^{114}Cd and ^{116}Cd data from this station are thus very likely incorrect. On the other hand, owing to the fact that the ^{110}Cd/^{111}Cd ratio is free of interference and that all the other aspects of the protocol are validated, this single ratio allows determination of the Cd IC at this site.

3.4. Measurement of Cd Concentrations

To determine Cd concentrations in the seawater samples, 3 mL of unfiltered seawater was spiked with ^{108}Cd, evaporated, loaded onto the AGMP1 column and eluted following the protocol described above (section 3.1.2.). The Cd concentrations were then determined by isotopic dilution on a

ThermoFinnigan Element II inductively coupled plasma mass spectrometer (ICPMS, WHOI). The total procedural blank was ~23 ± 3 pg (1σ). Blank variability sets the detection limit to 9 pg (defined as three times the blank standard deviation), which is less than a third of the Cd content of the most depleted sample. Duplicate analyses of seawater samples yielded an external reproducibility of 2% (2σ), equivalent to the internal precision of ~1.5% ($2\sigma_n$). The concentrations measured in the northwest Pacific and in the Mediterranean Sea were in very good agreement with Cd profiles measured earlier in neighboring areas (Bruland, 1980; Laumond et al., 1984).

4. RESULTS AND DISCUSSION

4.1. Seawater Cd isotopic data

$\varepsilon^{110/111}_{Cd/amu}$ profiles at station K1 and DYFAMED (Fig. 6) vary between -0.8 and +0.7 (similar values are found for the other ratios at K1). This range is more than one order of magnitude smaller than the variability found for light elements such as C, N and Si. It is similar to those reported in the single study published so far about Cu and Zn isotopes in seawater (northeast Pacific), ~0.15 and ~0.25‰ for δ^{66}Zn and δ^{65}Cu per atomic mass unit, respectively (Bermin et al., 2006). Apparent enrichment of the light isotopes of both Cd and Zn in biogenic particulate matter suggests qualitatively similar biochemical control and is consistent with the close association of these metals in living organisms, while the opposite fractionation for Cu suggests removal dominated by non-physiological scavenging processes. Although the measured Cd isotopic variability is barely larger than the mean uncertainty of measurement (0.8 $\varepsilon_{Cd/amu}$), there are hints of oceanographically consistent features in the seawater profiles, which can be tentatively interpreted.

4.1.1. Upper 300 m of the northwest Pacific station

The progressive $\varepsilon_{Cd/amu}$ decrease from the surface to 300 m depth at station K1 is associated with a Cd concentration increase, suggesting that the Cd isotopic ratios in the upper water column may be controlled by Rayleigh fractionation, driven by preferential uptake and removal of isotopically light Cd by phytoplankton:

$$\left(\varepsilon_{Cd/amu}\right)_{SW}^{f} = \left(\varepsilon_{Cd/amu}\right)_{SW}^{f=1} - \alpha \ln(f) \qquad (10)$$

$$\left(\varepsilon_{Cd/amu}\right)_{I-Pkt}^{f} = \left(\varepsilon_{Cd/amu}\right)_{SW}^{f} - \alpha \qquad (11)$$

$$\left(\varepsilon_{Cd/amu}\right)_{A-Pkt}^{f} = \left(\varepsilon_{Cd/amu}\right)_{SW}^{f=1} + \alpha \frac{f \times \ln(f)}{1-f} \qquad (12)$$

where f is the fraction of dissolved Cd remaining in solution and α is the fractionation factor per amu. The term $\left(\varepsilon_{Cd/amu}\right)_{X}^{f}$ is the $\varepsilon_{Cd/amu}$ value of media X for a given value of f. The subscripts SW, I-Pkt and A-Pkt subscript refer to seawater, instantaneous (I) and accumulated (A) phytoplankton products, respectively.

Rearranging equation (10) indicates that, in the case of Rayleigh distillation, there should be a linear relationship between the logarithm of the Cd concentration in seawater ($[Cd]_{SW}^{f}$) and its isotopic ratios, with the slope of the relationship equal to -α:

$$\left(\varepsilon_{Cd/amu}\right)_{SW}^{f} = \left(\varepsilon_{Cd/amu}\right)_{SW}^{f=1} + \alpha \ln[Cd]_{SW}^{f=1} - \alpha \ln[Cd]_{SW}^{f} \qquad (13)$$

The Cd depletion in K1 surface water (30 m depth) reaches ~56% relative to the subsurface Cd concentration maximum (300 m depth). Despite large uncertainties, we find a linear relationship between Cd IC and the logarithm of Cd concentration (Fig. 8). These results suggest that the Cd isotopic variation measured between the surface and 300 m depth may be due to Rayleigh distillation induced by phytoplankton uptake and sinking, following presumed Cd input events, for example through upwelling or winter mixing. The fractionation factor estimated from the linear regression of the data is α= 1.6±1.4

$\varepsilon_{Cd/amu}$ units for $\varepsilon^{110/111}_{Cd/amu}$ and α= 1.5±1.4 for $\varepsilon^{114/111}_{Cd/amu}$, ignoring the 2% uncertainty of the concentration data, and taking a Cd IC uncertainty of 0.8 $\varepsilon_{Cd/amu}$ unit.

4.1.2. 300-700 m layer of the northwest Pacific station

Below the upper 300 meter layer, there is a progressive $\varepsilon_{Cd/amu}$ increase from $\varepsilon^{110/111}_{Cd/amu}$=-0.9±0.8 (300 m depth) to $\varepsilon^{110/111}_{Cd/amu}$=0.5±0.8 at 700 m depth. This increase is not associated with significant Cd concentration variations (cf. Fig. 2 and Table 3).

The potential temperature profile (Fig. 9) documents a maximum at ~300 m depth, corresponding to the mesothermal water (Uda, 1963), which originates from the area east of Japan (Ueno and Yasuda, 2000, , 2003). Below this water mass, a well developed oxygen minimum and nitrate maximum, centered around 600 m (Fig. 9), clearly identifies the North Pacific Intermediate Water. A silicate maximum centered at 2000 m depth identifies the North Pacific Deep Water. The $\varepsilon_{Cd/amu}$ increase from 300 m to 700 m depth could therefore reflect the mixing between the mesothermal water and the North Pacific Intermediate Water. In such a case, the product of $\varepsilon^{110/111}_{Cd/amu}$ and the Cd concentration should behave conservatively within this depth range. Fig. 10 displays this quantity versus salinity. Despite the large uncertainties of these data, their mean values are strongly linearly correlated between 300 and 700 m depth (correlation coefficient R=0.99, significance level P<0.001), which suggests that $\varepsilon^{110/111}_{Cd/amu} \times [Cd]$ behaves conservatively within this depth range (similar relationships, not shown here for clarity purpose, are found for $\varepsilon^{110/111}_{Cd/amu} \times [Cd]$ versus potential temperature and nitrate, phosphate and silicate concentrations, with (R=-0.96, P=0.04), (R=-0.99, P=0.01), (R=-0.99, P=0.01), and (R=0.99 and P=0.004), respectively). Again, despite the large uncertainties of the Cd isotopic data, this observation suggests that the Cd isotopic composition variation observed between the core of the mesothermal water (300 m depth) and the core of the North Pacific Intermediate Water (700 m depth) is the result of water mass mixing.

Below this depth, no significant Cd isotopic composition variation is found; in particular, no distinctive signature is associated with the North Pacific Deep Water.

4.1.3. Northwest Mediterranean station

The range of variation at this site (1.3 $\varepsilon_{Cd/amu}$ unit; Fig. 6b) is comparable to that found in the North Pacific. However, in contrast to the North Pacific, we could not find statistically significant relationships between the Cd IC and any of the following parameters: Cd concentration (which could have supported the hypothesis of a Rayleigh distillation), the conservative tracers (θ and S, which could have supported the hypothesis of a water mass mixing), the nutrient and dissolved oxygen concentrations.

The lack of measurable Cd isotopic fractionation due to Rayleigh distillation is not surprising considering the relatively small Cd depletion at the surface (~27% depletion relative to the subsurface maximum, located at 100 m depth, at the base of the seasonal thermocline). Using the fractionation factor calculated in the North Pacific surface waters (α=1.6), the DYFAMED surface depletion would result in a Cd IC increase of 0.5 $\varepsilon_{Cd/amu}$ unit (-1.6xLn(0.73)=0.5, cf. equation 10), which is within measurement uncertainty.

There are three distinct water masses at the DYFAMED site: Modified Atlantic Water, Levantine Intermediate Water (θ and S local maximum around 300 to 400 m depth) originating from the Eastern Mediterranean Sea, and Western Mediterranean Deep Water (θ≈12.8°C and S≈38.45) (Millot, 1999). Between 400 and 2000 m depth, a linear relationship between θ and S (R^2=0.99, not shown, cf. Table 3) clearly indicates mixing between the Levantine Intermediate Water and Western Mediterranean Deep Water. Therefore, the DYFAMED water column is clearly composed of water masses from different origins that mix together. The lack of measurable Cd isotopic variation associated to this hydrographic setting therefore suggests that these three water masses have similar Cd IC (within the measurement uncertainty). This homogeneity could result from deep water formation processes in the Mediterranean Sea. This hypothesis is supported by Boyle et al (1985), who suggested that comparable trace metal (including Cd) levels found in deep Mediterranean waters and in surface waters in regions of Mediterranean deep water formation imply a minimal role for trace metal transport by biological activity relative to deep water formation processes.

4.2. Culture experiment

Cadmium isotopic data from the phytoplankton culture experiment are reported in Table 4. Sn interference corrections (cf. section 3.2.1) were too large for accurate measurements of ^{116}Cd and ^{112}Cd . Interference correction anomalies (as defined in section 3.2.1.) for ^{114}Cd were lower than or equal to 1.1 $\varepsilon_{Cd/amu}$ unit. The ^{114}Cd/^{111}Cd ratio of the phytoplankton samples will thus be cautiously used in the following, in addition to the interference-free ^{110}Cd/^{111}Cd ratio. The ^{114}Cd/^{111}Cd and ^{110}Cd/^{111}Cd ratio data (Fig. 11) are in excellent agreement for the Cd-powder, Stock-solution and Cultured-solution samples, for which the Sn interferences were low, and in fairly good agreement for the phytoplankton samples (subject to larger Sn interferences).

Since less than 1% of total Cd in the media was removed by phytoplankton uptake during the incubation, we assume that the Cd IC of the media did not change during phytoplankton growth. The initial Cd isotopic composition of the culture media before the growth experiment could therefore equally be determined from the Cd powder, stock solution or cultured solution samples (cf. Fig. 11). These three samples have similar Cd IC (cf. Fig. 11 and Table 4). However, the initial Cd isotopic composition of the culture media was determined as the mean value of the Cd powder and stock solution samples, because these samples are more concentrated than the cultured solution sample, and therefore provide a more reliable measurement: $\varepsilon^{110/111}_{Cd/amu}$=-2.3±0.8 (2σ; $\varepsilon^{114/111}_{Cd/amu} = -2.7 \pm 1.1$). The phytoplankton samples have a mean value of $\varepsilon^{110/111}_{Cd/amu}$=-5.7±1.2 (2σ ; $\varepsilon^{114/111}_{Cd/amu} = -4.7 \pm 1.5$). The significant difference between the initial Cd IC of the culture media and that of the phytoplankton suggest that the phytoplankton preferentially take up light Cd isotopes. Less than 1% Cd was taken up from the culture media by the cells. Neglecting this depletion, equation 11 (instantaneous product) yields a fractionation factor α=3.4±1.4 $\varepsilon_{Cd/amu}$ units (2σ, from the ^{110}Cd/^{111}Cd ratios; α=2.0±1.9 $\varepsilon_{Cd/amu}$ units from the ^{114}Cd/^{111}Cd ratios; using equation 12 with f=0.99 gives the same results). These values are comparable (given the uncertainties) to those derived from the northwest Pacific seawater samples (α=1.6±1.4 $\varepsilon_{Cd/amu}$ units). The difference between the phytoplankton uptake fractionation factor and that derived from the water column distributions may

be the result of a number of factors including non-representative phytoplankton species or growth rate, Cd scavenging in the water column by particle adsorption in addition to biological uptake, inappropriate assumptions in application of the Rayleigh fractionation model, or IC measurement uncertainty. Further research will be required to further constrain the processes leading to Cd isotope variations in the oceanic water column.

5. SUMMARY AND CONCLUDING REMARKS

The range of cadmium isotopic composition (Cd IC) in seawater from the northwest Pacific and the northwest Mediterranean is not greater than 1.5 $\varepsilon_{Cd/amu}$ units. It is only slightly larger than the mean uncertainty of measurement using the method described here (0.8 $\varepsilon_{Cd/amu}$) and more than one order of magnitude smaller than the variability found for light elements such as C, N and Si. On the other hand, it is very similar to those reported in the single study published so far about Cu and Zn isotopes in seawater (northeast Pacific. Bermin et al., 2006).

In the northwest Pacific station, despite error bars approaching the measured isotopic variability, we find systematic relationships between the Cd IC and Cd concentration in the upper 300m, and between Cd IC and hydrographic data between 300 and 700m. These results suggest that i) the variation observed within the upper 300 m layer may be due to Cd isotopic fractionation by phytoplankton uptake, with a fractionation factor of 1.6±1.4 $\varepsilon_{Cd/amu}$ units; ii) the variation observed between 300 and 700 m depth, may be due to the mixing of the mesothermal water ($\varepsilon^{110/111}_{Cd/amu}$=-0.9±0.8) with the North Pacific Intermediate Water ($\varepsilon^{110/111}_{Cd/amu}$=0.5±0.8).

On the other hand, at the DYFAMED site (Mediterranean), we cannot find similar correlations between Cd IC and Cd concentration nor between the Cd IC and hydrographic data. We suggest that this lack of systematic Cd IC variation is due to i) insufficient surface Cd depletion by phytoplankton uptake in the surface waters and ii) similar Cd IC of the different water masses found at this site, possibly linked to deep water formation processes.

Culture experiments suggest that freshwater phytoplankton (*Chlamydomonas reinhardtii* and *Chlorella*) preferentially take up light Cd isotopes, with a fractionation factor of 3.4±1.4 $\varepsilon_{Cd/amu}$ units (similar fractionation is found for both species). This observation supports the conclusion based on the NW Pacific data that biological uptake of Cd by phytoplankton results in a small preferential uptake of the lighter Cd isotopes.

The North Pacific data suggest that different water masses may have different Cd IC, notably the mesothermal water with $\varepsilon_{Cd/amu}^{110/111} \sim$ -1 compared to ~ 0.3 for deeper waters. The present data set is insufficient to establish the origin of this signature but suggests that Cd isotopes could provide information on water mass trajectory and mixing in some areas of the ocean.

Future studies aimed at quantifying specific Cd isotopic fractionations associated with various aspects of biological uptake, adsorptive scavenging and remineralization of organic matter may provide new insight into these processes. Understanding controls on the mean Cd isotope composition of the ocean will require measurements of the mean river input Cd IC and of fractionations associated with ultimate Cd removal in organic-rich and reducing sediments. Investigations of Cd isotope distributions and mean IC in the past ocean, while technically difficult, may help to quantify past changes in the oceanic budget, internal cycling, and advective transport of this element, augmenting the current paleoceanographic utility of cadmium. The small variations in Cd isotopic composition found in this study indicate that applications of this parameter for studying the present or past Cd oceanic cycle will be challenging. This will likely require further analytical improvements. Better precision could likely be obtained with larger seawater samples, a better chemical separation of tin and a more accurate mass bias correction through the use of the double spiking technique.

Acknowledgements. We thank K. Bruland for his advice about chemical procedures. We acknowledge O. Rouxel and C. Cloquet for their help with the chromatography. We are grateful to L. Ball for his help with the MC-ICPMS. C. Jeandel is acknowledged for providing the Mediterranean seawater samples, and

P. van Beek and M. Kienast for carrying out the sampling of the Pacific samples. We thank H. de Baar and two anonymous reviewers for very helpful comments that improved this manuscript.

References

Abe K. (2002) Preformed Cd and PO4 and the relationship between the two elements in the northwestern Pacific and the Okhotsk Sea. *Mar. Chem.* **79** 27- 36.

Bermin J., Vance D., Archer C., and Statham P. J. (2006) The determination of the isotopic composition of Cu and Zn in seawater. *Chem. Geol.* **226**(3-4), 280-297.

Boyle E. A. (1988) Cadmium: chemical tracer of deepwater paleoceanography. *Paleoceanography* **3**, 471-489.

Boyle E. A., Chapnick S. D., Bai X. X., Spivack A., and Huested S. S. (1985) Trace metal enrichments in the Mediterranean Sea. *Earth Planet. Sci. Lett.* **74**, 405-419.

Boyle E. A., Sclater F., and Edmond J. M. (1976) On the marine geochemistry of cadmium. *Nature* **263**, 42-44.

Bruland K. (1980) Oceanographic distributions of cadmium, zinc, nickel, and copper in the North Pacific. *Earth Planet. Sci. Lett.* **47**, 176-198.

Bruland K. W., Knauer G. A., and Martin J. H. (1978) Cadmium in northeast Pacific waters. *Limnol. Oceanogr.* **23**, 618-625.

Cullen J. T. (2006) On the nonlinear relationship between dissolved cadmium and phosphate in the modern global ocean: Could chronic iron limitation of phytoplankton growth cause the kink? *Limnol. Oceanogr.* **51**(3), 1369-1380.

Cullen J. T., Chase Z., Coale K. H., Fitzwater S. E., and Sherrell R. M. (2003) Effect of iron limitation on the cadmium to phosphorus ratio of natural phytoplankton assemblages from the Southern Ocean. *Limnol. Oceanogr.* **48**(3), 1079-1087.

Cullen J. T., Lane T. W., Morel F. M. M., and Sherrell R. M. (1999) Modulation of cadmium uptake in phytoplankton by seawater CO_2 concentration. *Nature* **402**, 165-167.

Elderfield H. and Rickaby R. E. M. (2000) Oceanic Cd/P ratio and nutrient utilization in the glacial Southern Ocean. *Nature* **405**, 305-310.

Frew R., Bowie A., Croot P., and Pickmere S. (2001) Macronutrient and trace-metal geochemistry of an in situ iron-induced Southern Ocean bloom. *Deep Sea Res. II* **48**(11-12), 2467.

Frew R. D. and Hunter K. A. (1992) Influence of Southern Ocean waters on the Cd-phosphate properties of the global ocean. *Nature* **360**, 144-146.

Helmers E. (1996) Trace metals insuspended particulate matter of Atlantic Ocean surface water (40°N to 20°S). *Mar. Chem.* **53**, 51-67.

Kingston H. M., Barnes I. L., Brady T. J., and Rains T. C. (1978) Separation of eight transition elements from alkali and alkaline earth elements in estuarine and seawater with chelating resin and their determination by graphite furnace atomic adsorption spectrometry. *Anal. Chem.* **50**, 2064-2070.

Lane T. W., Saito M. A., George G. N., Pickering I. J., Prince R. C., and Morel F. M. M. (2005) A cadmium enzyme from a marine diatom. *Nature* **435**(7038), 42-42.

Laumond F., Copin-Montegut G., Courau P., and Nicolas E. (1984) Cadmium, copper and lead in the Western Mediterranean Sea. *Mar. Chem.* **15**, 251-261.

Marechal C. N., Telouk P., and Albarede F. (1999) Precise analysis of copper and zinc isotopic compositions by plasma-source mass spectrometry. *Chem. Geol.* **156**, 251–273.

Martin J. H., Gordon R. M., S.F. F., and Broenkow W. W. (1989) VERTEX: phytoplankton/iron studies in the Gulf of Alaska. *Deep-Sea Res.* **36**, 649-680.

Millot C. (1999) Circulation in the Western Mediterranean Sea. *Journ. Mar. Sys.* **20**, 432-442.

Morel F. M. M., Reinfelder J. R., Roberts S. B., Chamberlain C. P., Lee J. G., and Yee D. (1994) Zinc and carbon co-limitation of marine phytoplankton. *Nature* **369**, 740-742.

Pai S. C., Chen T. C., Wong G. T. F., and Hung C. C. (1990) Maleic acid/ammonium hydroxide buffer system for preconcentration of trace metals from seawater. *Anal. Chem.* **62**(7), 774 - 777.

Price N. M. and Morel F. M. M. (1990) Cadmium and cobalt substitution for zinc in a marine diatom. *Nature* **344**, 658-660.

Riso R. D., Le Corre P., L'Helguen S., and Morin P. (2004) On the presence of a cadmium-rich subsurface water mass in the western Mediterranean and its influence on the distribution of cadmium in the surface waters. *Mar. Chem.* **87**(1-2), 15-22.

Rosman K. J. R. and Taylor P. D. P. (1998) Isotopic compositions of the elements 1997. *Pure and Applied Chemistry* **70**(1), 217-235.

Russel W. A., Papanastassiou D. A., and Tombrello T. A. (1978) Ca isotope fractionation on the Earth and other solar system materials. *Geochim. Cosmochim. Acta* **42**, 1075–1090.

Sherrell R. M. (1989) The trace metal geochemistry of suspended oceanic particulate matter. Ph-D Thesis, MIT-WHOI (USA), 211 p.

Sunda W. G. and Huntsman S. A. (2000) Effect of Zn, Mn, and Fe on Cd accumulation in phytoplankton: implications for oceanic Cd cycling. *Limnol. Oceanogr.* **45**, 1501– 1516.

Uda M. (1963) Oceanography of the Subarctic Pacific Ocean. *J. Fish. Res. Board Can.* **20**, 119-179.

Ueno H. and Yasuda I. (2000) Distribution and formation of the mesothermal structure (temperature inversions)in the North Pacific subarctic region. *J. Geophys. Res.* **105**(C7), 16885-16897.

Ueno H. and Yasuda I. (2003) Intermediate water circulation in the North Pacific subarctic and northern subtropical regions. *J. Geophys. Res.* **108**(C11), doi:10.1029/2002JC001372.

van Geen A., Boyle E. A., and Moore W. S. (1991) Trace metal enrichments in the waters of the Gulf of Cadiz. *Geochim. Cosmochim. Acta* **55**, 2173-2191.

Wombacher F. and Rehkämper M. (2004) Problems and Suggestions Concerning the Notation of Cadmium Stable Isotope Compositions and the Use of Reference Materials. *Geostand. Geoanal. Res.* **28**(1).

Wombacher F., Rehkamper M., Mezger K., and Munker C. (2003) Stable isotope compositions of cadmium in geological materials and meteorites determined by multiple-collector ICPMS. *Geochim. Cosmochim. Acta* **67**(23), 4639–4654.

Table 1. Faraday cup configuration and isotopic abundances of Cd and of the elements that can produce isobaric interferences with Cd.

Nominal mass		105	106	107	108	109	110	111	112	113	114	115	116	117
Isotope abundance (%)	Pd	22.3	27.3		26.5		11.7							
	Ag			51.8		48.2								
	Cd		1.2		0.89		12.5	12.8	24.1	12.2	28.7		7.49	
	In									4.3		95.7		
	Sn								0.97		0.65	0.36	14.5	7.68
Collector configuration				L_4	L_3	L_2	L_1	C	H_1		H_2		H_3	H_4

Table 2. MC-ICPMS Cd operation parameters.

ThermoFinnigan Neptune at the Woods Hole Oceanographic Institution	
Standard conditions for Cd analysis	
RF Power	1200W
Acceleration voltage	10kV
Mass analyzer pressure	$5x10^{-9}$ millibar
Nebulizer	ESI PFA 50 [(a)]
Spray chamber	ESI SIS (Stable Introduction System) [(a)]
Sample uptake rate	~60 µL/min
Extraction lens	-2000 V
Typical signal intensity	~2.3 nA/ppmCd [(b)]
Transmission efficiency	~0.04%
Mass Discrimination	~1.4% per amu
Desolvating Sample Introduction System (Cetac® Aridus)	
Nebulizer	ESI PFA 50 [(a)]
Spray chamber	ESI PFA Teflon upgrade [(a)]
Spray chamber temperature	100°C
Desolvating membrane temperature	70°C
Sample uptake rate	~60 µL/min
Argon sweep gas flow	~6 L/min (optimized for max. signal)
Nitrogen additional gas	~10 mL/min (optimized for sensitivity)

(a) ESI = Elemental Scientific Inc., Omaha, NB, USA.
(b) Based on 0.6 volt ^{110}Cd per 20ppb total Cd; 10^{11} ohm resistor

Table 3: Temperature, salinity, potential density, dissolved oxygen, nutrient and cadmium concentrations, and cadmium isotopic compositions of seawater samples from K1 (northwest Pacific) and DYFAMED (northwest Mediterranean - The nutrient concentrations at DYFAMED were measured on 10/07/2003, 2 weeks after the Cd sampling) stations. A few nutrient concentrations reported in italic are linear interpolation of nearby data.

Sample	θ (°C)	S	σ_θ (kg/m3)	O_2 (µmol/kg)	NO_3 (µmol/kg)	$Si(OH)_4$ (µmol/kg)	PO_4 (µmol/kg)	Cd (nmol/L)	$\varepsilon^{110/111}_{Cd/amu}$	$\varepsilon^{112/111}_{Cd/amu}$	$\varepsilon^{114/111}_{Cd/amu}$
K1 - 30 m [a]	8.04	32.88	25.60	293.33	15.0	28.7	1.35	0.489	0.4	0.7	0.5
K1 - 60 m	2.19	33.09	26.42	318.43	*22.0*	*37.3*	*1.81*	0.768	-0.2	0.5	0.2
K1 - 100 m	1.32	33.14	26.53	308.61	26.2	43.3	2.01	0.747	-0.1	0.1	0.0
K1 - 123 m [a]	1.50	33.28	26.63	264.70	29.9	53.8	2.24	0.821	-0.2	0.0	-0.1
K1 - 300 m [a]	3.49	34.02	27.06	27.07	44.4	107.8	3.13	1.105	-0.9	-0.8	-0.8
K1 - 400 m [a]	3.41	34.13	27.15	22.74	44.2	117.4	3.11	1.057	-0.4	-0.8	-0.4
K1 - 500 m [a]	3.25	34.22	27.24	20.97	44.0	124.8	3.10	1.038	0.0	-0.2	-0.1
K1 - 700 m	2.95	34.31	27.34	20.64	*43.9*	*137.0*	*3.09*	1.046	0.5	1.0	0.5
K1 - 900 m	2.65	34.39	27.43	23.58	*43.8*	*147.9*	*3.09*	1.037	0.2	0.7	0.5
K1 - 1000 m	2.51	34.43	27.47	24.98	43.8	153.2	3.09	1.038	0.2	0.5	0.2
K1 - 1250 m [a]	2.23	34.49	27.55	34.50	*43.1*	*158.9*	*3.03*	1.041	0.2	0.3	0.2
K1 - 1500 m	2.01	34.54	27.60	47.11	42.4	165.1	2.98	1.016	0.6	0.9	0.7
K1 - 2000 m	1.70	34.60	27.68	73.94	40.6	167.1	2.85	0.985	0.3	0.6	0.4
K1 - 3000 m	1.33	34.66	27.75	121.37	37.6	157.8	2.61	0.893	0.1	0.5	0.4
K1 - 4000 m [a]	1.15	34.68	27.78	144.30	36.2	150.5	2.48	0.879	0.3	0.5	0.3
K1 - 5000 m	1.09	34.69	27.79	152.28	35.6	150.3	2.44	0.831	0.1	0.6	0.4
DYF - 20 m	15.90	38.27	28.29	259.85	0.00	0.63	0.00	0.065	-0.6	-	-
DYF - 50 m	13.32	38.30	28.89	254.43	3.47	1.46	0.06	0.069	-0.5	-	-
DYF - 75 m	13.21	38.35	28.95	199.04	*6.34*	*2.75*	*0.23*	0.086	-0.5	-	-
DYF - 100 m	13.21	38.40	28.98	194.99	*7.13*	*3.34*	*0.29*	0.088	0.1	-	-
DYF - 150 m	13.35	38.49	29.03	179.63	7.65	4.11	0.33	0.084	0.7	-	-
DYF - 200 m	13.39	38.53	29.05	174.09	8.03	5.89	0.31	0.085	0.2	-	-
DYF - 300 m	13.44	38.58	29.08	164.96	8.99	6.75	0.33	0.084	-0.4	-	-
DYF - 400 m	13.38	38.58	29.09	165.98	8.99	7.73	0.38	0.081	0.6	-	-
DYF - 800 m	13.17	38.54	29.10	177.47	8.35	8.04	0.40	0.073	-0.6	-	-
DYF - 1200 m	12.97	38.49	29.10	183.38	*8.34*	*7.82*	*0.39*	0.072	0.0	-	-
DYF - 1500 m	12.87	38.46	29.10	187.63	5.54	4.91	0.24	0.075	-0.5	-	-
DYF - 2000 m	12.82	38.45	29.11	190.72	5.15	5.22	0.24	0.076	0.4	-	-

(a) samples for which replicate have been measured. In that case, the mean $\varepsilon_{Cd/amu}$ values are reported. Note that the DYFAMED $^{110}Cd/^{111}Cd$ data could not be validated by other Cd isotopic ratios (due to unsatisfactorily Sn interference corrections) and need therefore to be considered very cautiously.

Table 4: Cadmium isotopic composition of different phases involved in the phytoplankton culture experiment (cf. Fig. 11 caption for sample descriptions). Some $\varepsilon^{112/111}_{Cd/amu}$ data are not reported due to unsatisfactory Sn interference correction on ^{112}Cd.

Sample	$\varepsilon^{110/111}_{Cd/amu}$	$\varepsilon^{112/111}_{Cd/amu}$	$\varepsilon^{114/111}_{Cd/amu}$
Cd-Powder	-2.5	-3.2	-3.1
Stock-solution	-2.0	-2.3	-2.3
Cultured-solution	-3.1	-2.7	-2.7
Chlamydomonas-1	-6.6	-	-5.7[a]
Chlamydomonas-2	-5.7	-	-4.7[a]
Chlorella-1	-5.2	-	-4.4[a]
Chlorella-2	-5.2	-	-3.8[a]

(a) These data need to be used cautiously because of imperfect Sn interference corrections (see text for more details).

Figure Captions

Figure 1: The locations of the two sampling sites, shown by crosses.

Figure 2: Cd and phosphate profiles at the two sites. The nutrient concentrations at DYFAMED were measured on 10/07/2003, 2 weeks after the Cd sampling. The Cd error bars correspond to the internal precision (~3% at DYFAMED and 1.5% at K1, $2\sigma_n$), found to be similar to the reproducibility (2%).

Figure 3: Tin interference corrected and uncorrected data during one measurement session. The $\varepsilon_{Cd/amu}$ values are calculated relative to the mean JMC standard Cd ratios.

Figure 4: Instrumental mass fractionation corrections. Standard samples are indicated by large circles. The $\varepsilon_{Cd/amu}$ values are calculated relative to the mean JMC standard Cd ratios

Figure 5: Cadmium versus silver instrumental mass fractionation. Linear regressions for each measurement session, as well as for the whole data set are reported.

Figure 6: Cd isotopic composition profiles at station K1 (N.W. Pacific, a) and DYFAMED (N.W. Mediterranean Sea, b). Error bars represent the mean discrepancy between replicates (0.8 $\varepsilon_{Cd/amu}$ unit). Left panel: The different data series correspond to different measurement sessions (the mean profile is also displayed). Comparisons of these replicates allowed the determination of the reproducibility of the Cd IC measurement. The mean discrepancy between the duplicates is 0.8 $\varepsilon_{Cd/amu}$ unit, with a maximum discrepancy of 1.5 $\varepsilon_{Cd/amu}$ units (1250 m depth). Note that, because of the "/amu" notation, increasing values of $\varepsilon^{110/111}_{Cd/amu}$ reflect enrichment in heavy Cd isotopes.

Figure 7: Comparison of the isotopic compositions derived from different Cd isotope ratios at station K1 (N.W. Pacific). All isotopes were measured simultaneously. Error bars represent the mean discrepancy between replicates (0.8 $\varepsilon_{Cd/amu}$ unit). Note that the data from station DYFAMED (not shown for clarity purpose) do not show such inter isotope consistencies (because of unsatisfactory Sn interference corrections).

Figure 8: Cd isotopic composition versus the logarithm of the Cd concentration (nmol/L) in the surface layer of station K1 (upper 300m), for two Cd isotopic ratios ($^{110}Cd/^{111}Cd$ and $^{114}Cd/^{111}Cd$). Error bars correspond to 0.8 $\varepsilon_{Cd/amu}$ unit. Linear regressions are plotted. Their slopes (corresponding to the opposite of the Rayleigh fractionation factors, cf. equation 13), correlation coefficients (R) and significance levels (P) are reported. Note: the lower $\varepsilon_{Cd/amu}$ values correspond to lighter Cd.

Figure 9: Potential temperature, dissolved oxygen, nitrate and silicate concentrations and salinity at station K1. A detail of the upper 1000 m is displayed in the right panel.

Figure 10: Cd isotopic composition ($\varepsilon^{110/111}_{Cd/amu}$) times Cd concentration (nmol/L) versus salinity. The ellipse shows the linear relationship found between 300 and 700 m depth. The corresponding regression coefficient (R) and significance level (P) are indicated, as are some sampling depths. Errors bars are calculated by propagating the 0.8 $\varepsilon_{Cd/amu}$ unit uncertainty characterizing the Cd isotopic composition data (the 2% uncertainty of the concentration data are ignored).

Figure 11: Cadmium isotopic compositions (measured from $^{110}Cd/^{111}Cd$ and $^{114}Cd/^{111}Cd$ ratios) of different phases involved in the phytoplankton culture experiment. Cd-Powder: Cd used to make the Stock-solution; Stock-solution: initial solution used to grow the phytoplankton; Cultured-solution: growth media after culturing *Chlamydomonas* cells; Chlamydomonas 1 and 2: duplicate samples of *Chlamydomonas* cells; Chlorella 1 and 2: duplicate samples of *Chlorella* cells. Error bars correspond to 0.8 $\varepsilon_{Cd/amu}$ unit. Note: the lower $\varepsilon_{Cd/amu}$ values correspond to lighter Cd. Note also that $^{114}Cd/^{111}Cd$ ratios of the phytoplankton samples are imperfectly corrected for Sn interferences (see text for more details).

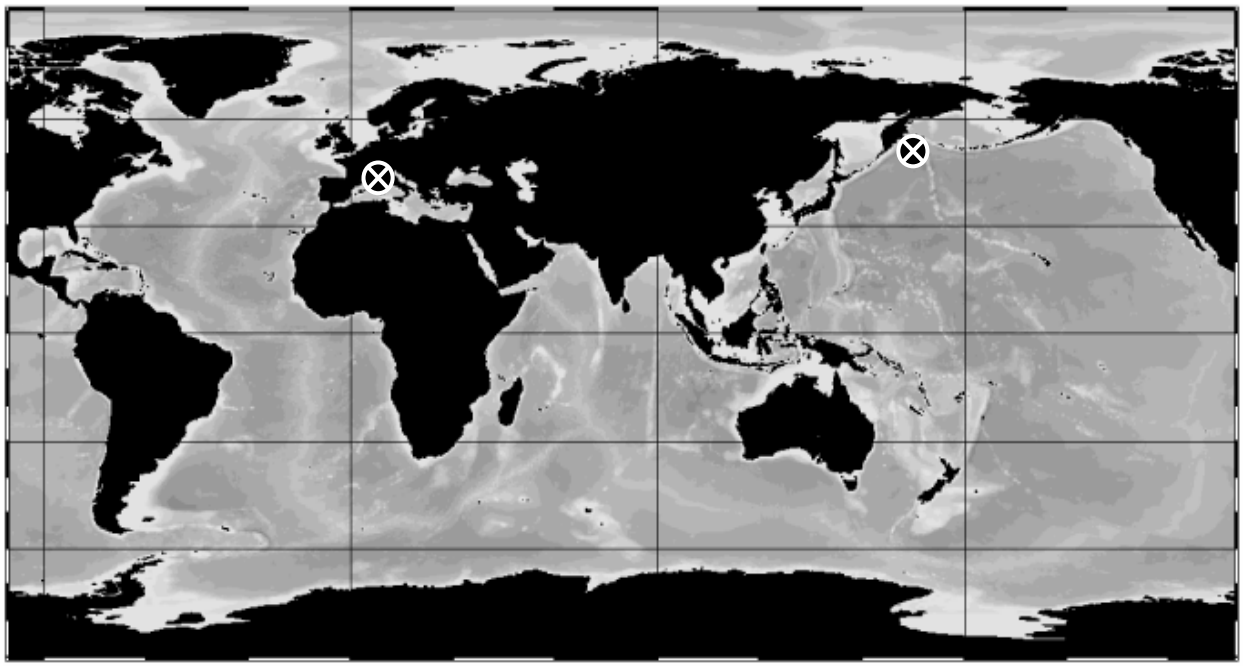

Figure 1

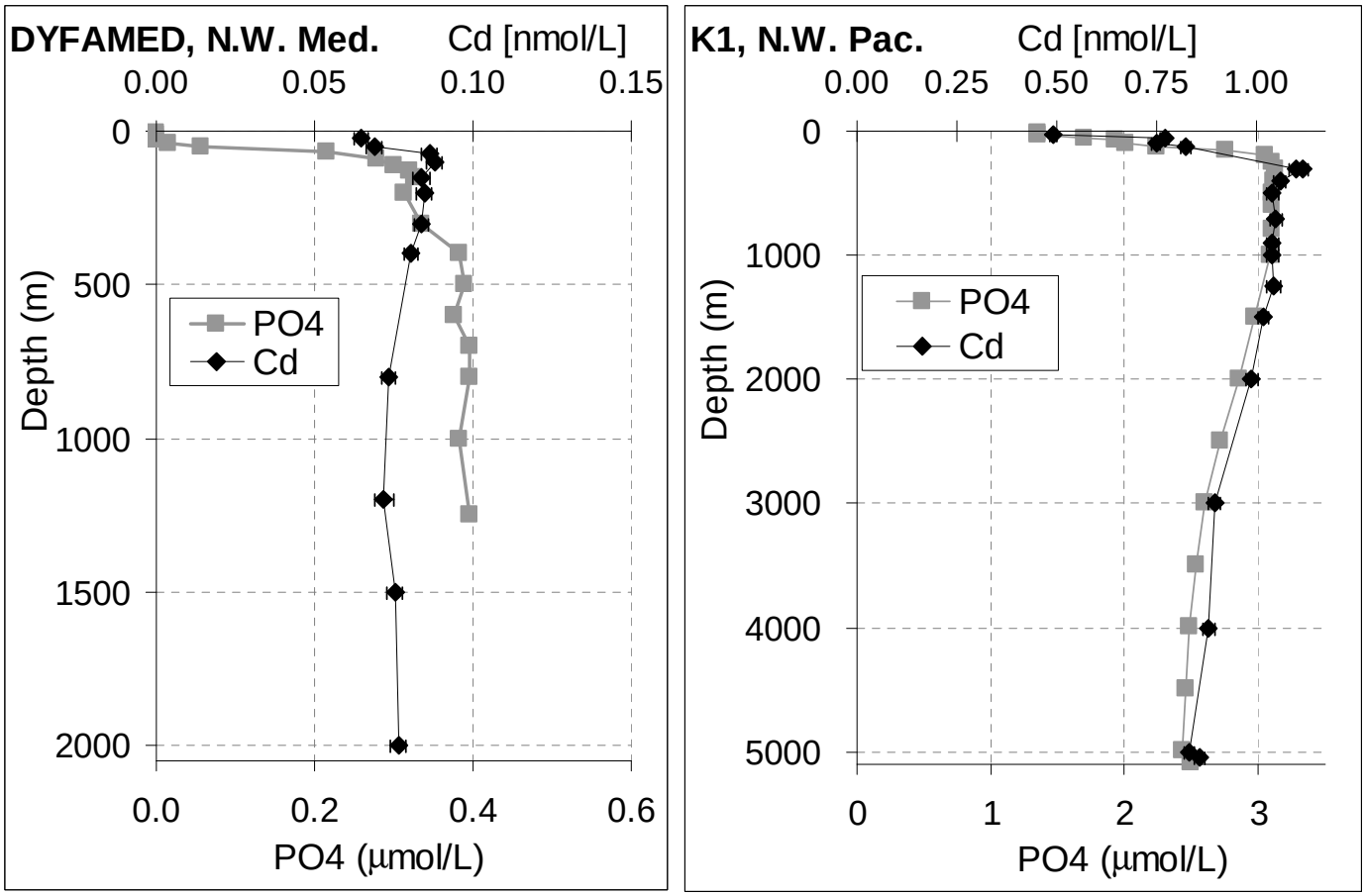
DYFAMED, N.W. Med.
Cd [nmol/L]
0.00
0.05
0.10
0.15
0
500
1000
1500
2000
Depth (m)
PO4
Cd
0.0
0.2
0.4
0.6
PO4 (µmol/L)
K1, N.W. Pac.
Cd [nmol/L]
0.00
0.25
0.50
0.75
1.00
0
1000
2000
3000
4000
5000
Depth (m)
PO4
Cd
0
1
2
3
PO4 (µmol/L)

Figure 2

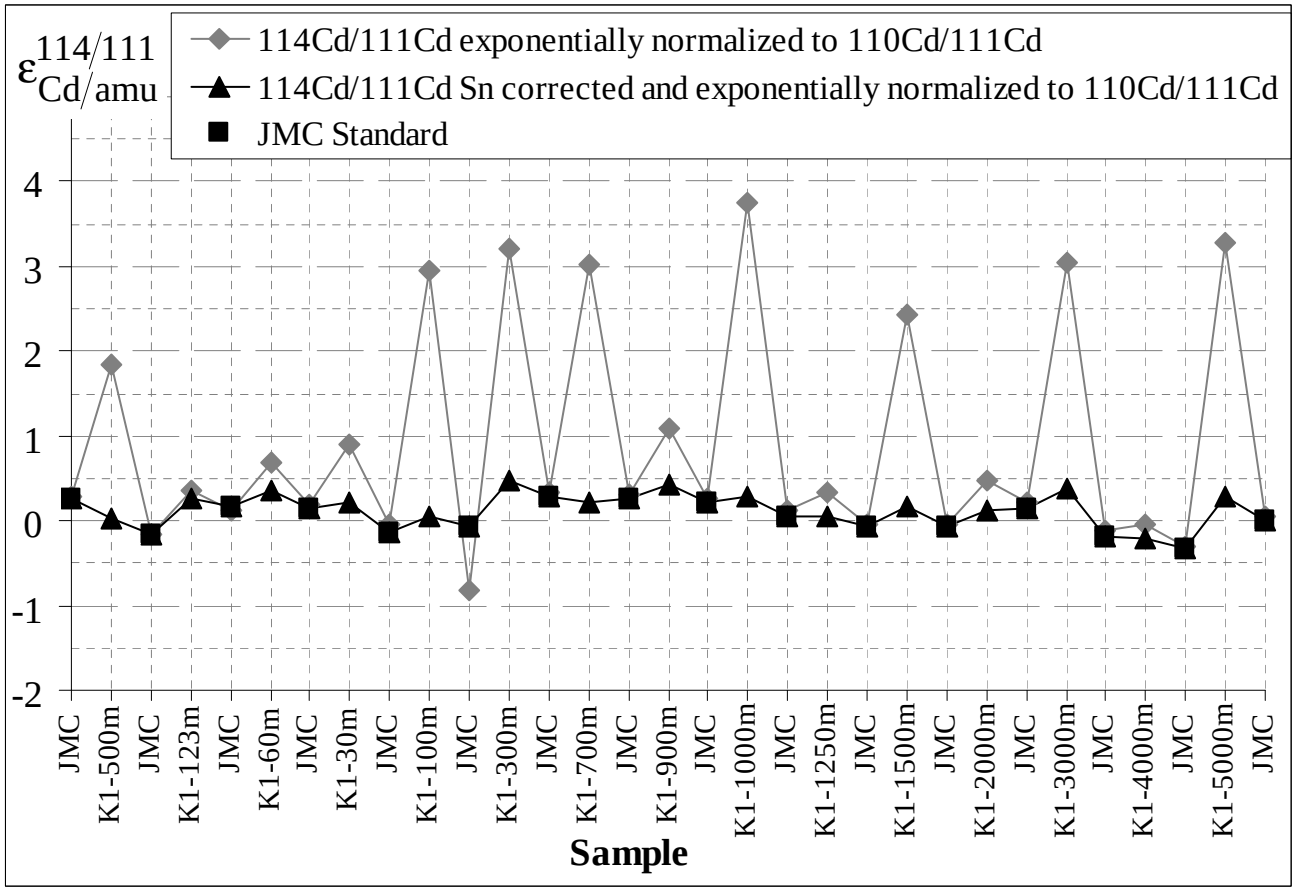
ε114/111 Cd/amu
114Cd/111Cd exponentially normalized to 110Cd/111Cd
114Cd/111Cd Sn corrected and exponentially normalized to 110Cd/111Cd
JMC Standard
4
3
2
1
0
-1
-2
JMC
K1-500m
JMC
K1-123m
JMC
K1-60m
JMC
K1-30m
JMC
K1-100m
JMC
K1-300m
JMC
K1-700m
JMC
K1-900m
JMC
K1-1000m
JMC
K1-1250m
JMC
K1-1500m
JMC
K1-2000m
JMC
K1-3000m
JMC
K1-4000m
JMC
K1-5000m
JMC
Sample

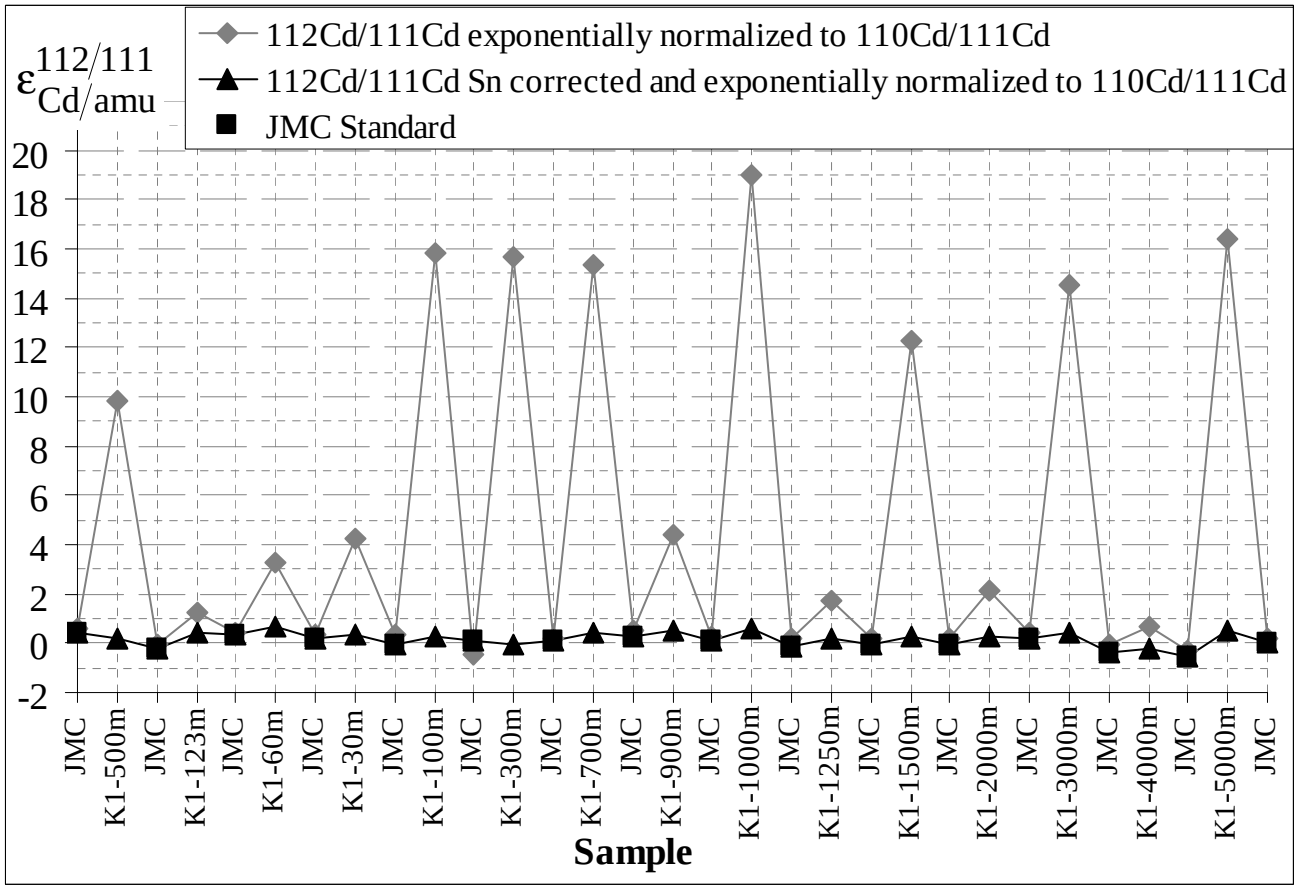
ε112/111 Cd/amu
112Cd/111Cd exponentially normalized to 110Cd/111Cd
112Cd/111Cd Sn corrected and exponentially normalized to 110Cd/111Cd
JMC Standard
20
18
16
14
12
10
8
6
4
2
0
-2
JMC
K1-500m
JMC
K1-123m
JMC
K1-60m
JMC
K1-30m
JMC
K1-100m
JMC
K1-300m
JMC
K1-700m
JMC
K1-900m
JMC
K1-1000m
JMC
K1-1250m
JMC
K1-1500m
JMC
K1-2000m
JMC
K1-3000m
JMC
K1-4000m
JMC
K1-5000m
JMC
Sample

Figure 3.

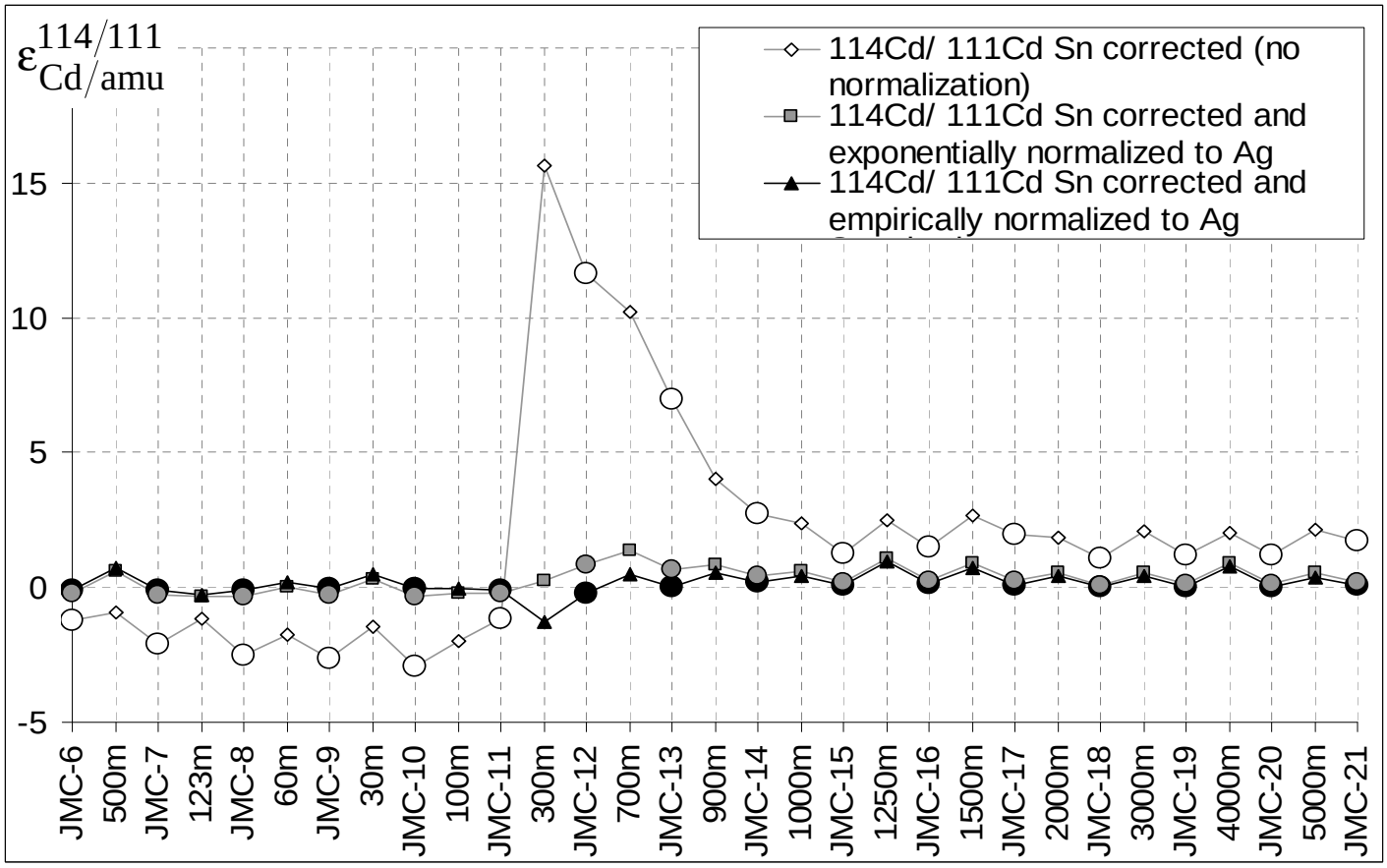
ε 114/111 Cd/amu
114Cd/ 111Cd Sn corrected (no normalization)
114Cd/ 111Cd Sn corrected and exponentially normalized to Ag
114Cd/ 111Cd Sn corrected and empirically normalized to Ag
15
10
5
0
-5
JMC-6
500m
JMC-7
123m
JMC-8
60m
JMC-9
30m
JMC-10
100m
JMC-11
300m
JMC-12
700m
JMC-13
900m
JMC-14
1000m
JMC-15
1250m
JMC-16
1500m
JMC-17
2000m
JMC-18
3000m
JMC-19
4000m
JMC-20
5000m
JMC-21

Figure 4.

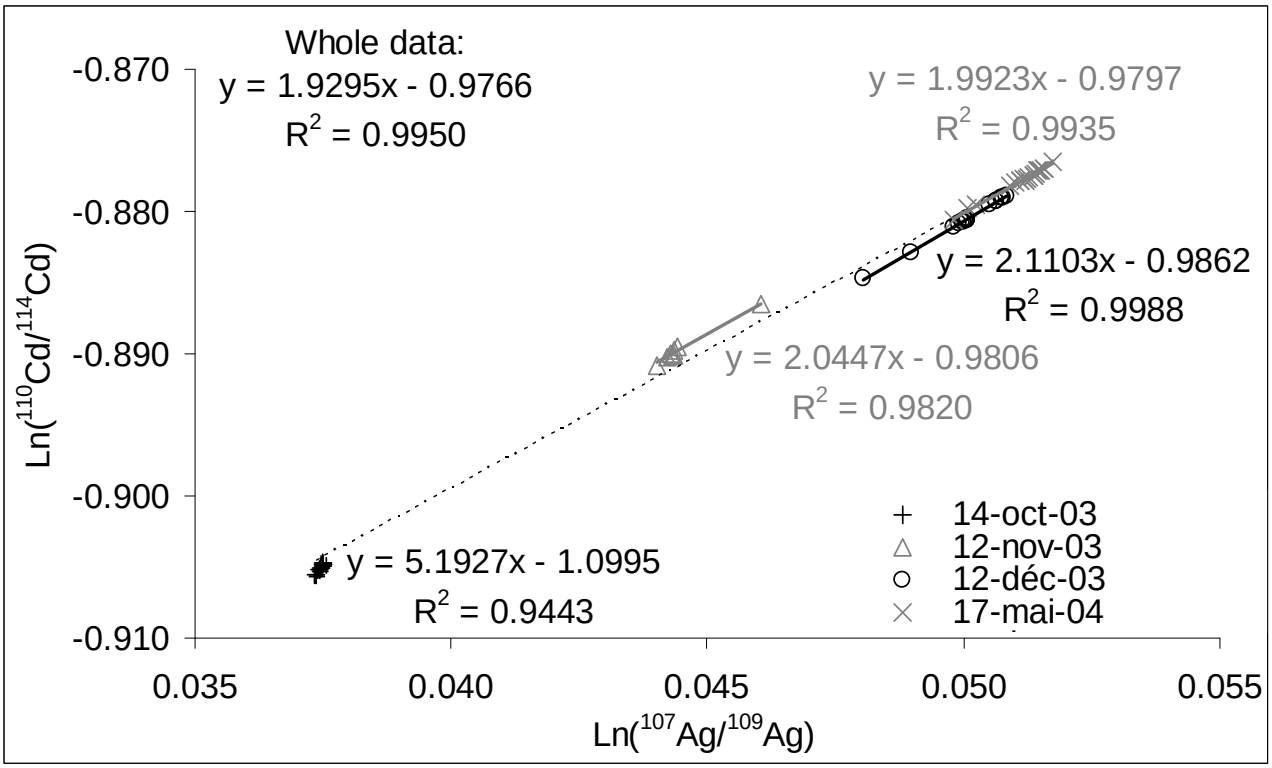
Whole data:
y = 1.9295x - 0.9766
R2 = 0.9950
y = 1.9923x - 0.9797
R2 = 0.9935
y = 2.1103x - 0.9862
R2 = 0.9988
y = 2.0447x - 0.9806
R2 = 0.9820
y = 5.1927x - 1.0995
R2 = 0.9443
14-oct-03
12-nov-03
12-déc-03
17-mai-04
-0.870
-0.880
-0.890
-0.900
-0.910
0.035
0.040
0.045
0.050
0.055
Ln(110Cd/114Cd)
Ln(107Ag/109Ag)

Figure 5

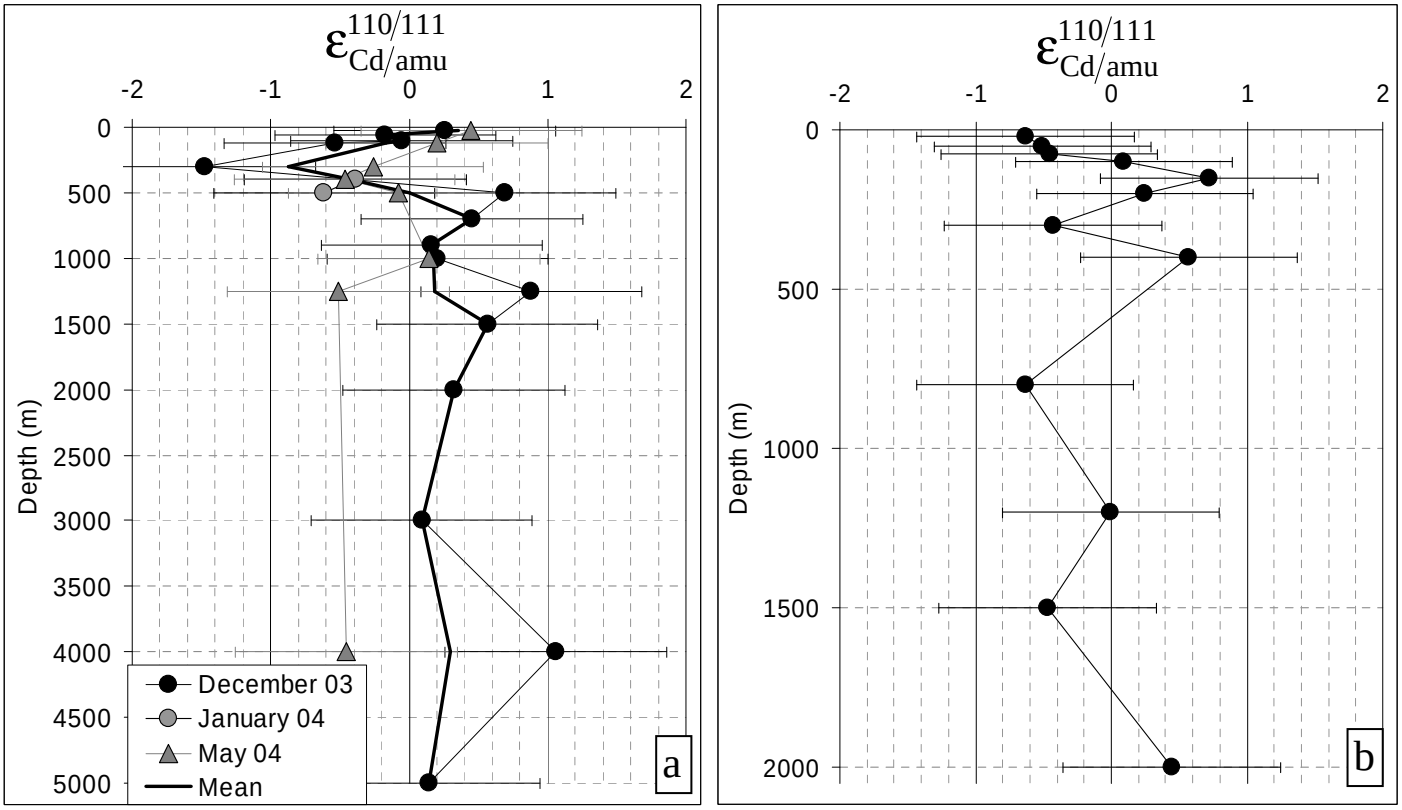
ε110/111 Cd/amu
-2
-1
0
1
2
Depth (m)
0
500
1000
1500
2000
2500
3000
3500
4000
4500
5000
December 03
January 04
May 04
Mean
a
ε110/111 Cd/amu
-2
-1
0
1
2
Depth (m)
0
500
1000
1500
2000
b

Figure 6

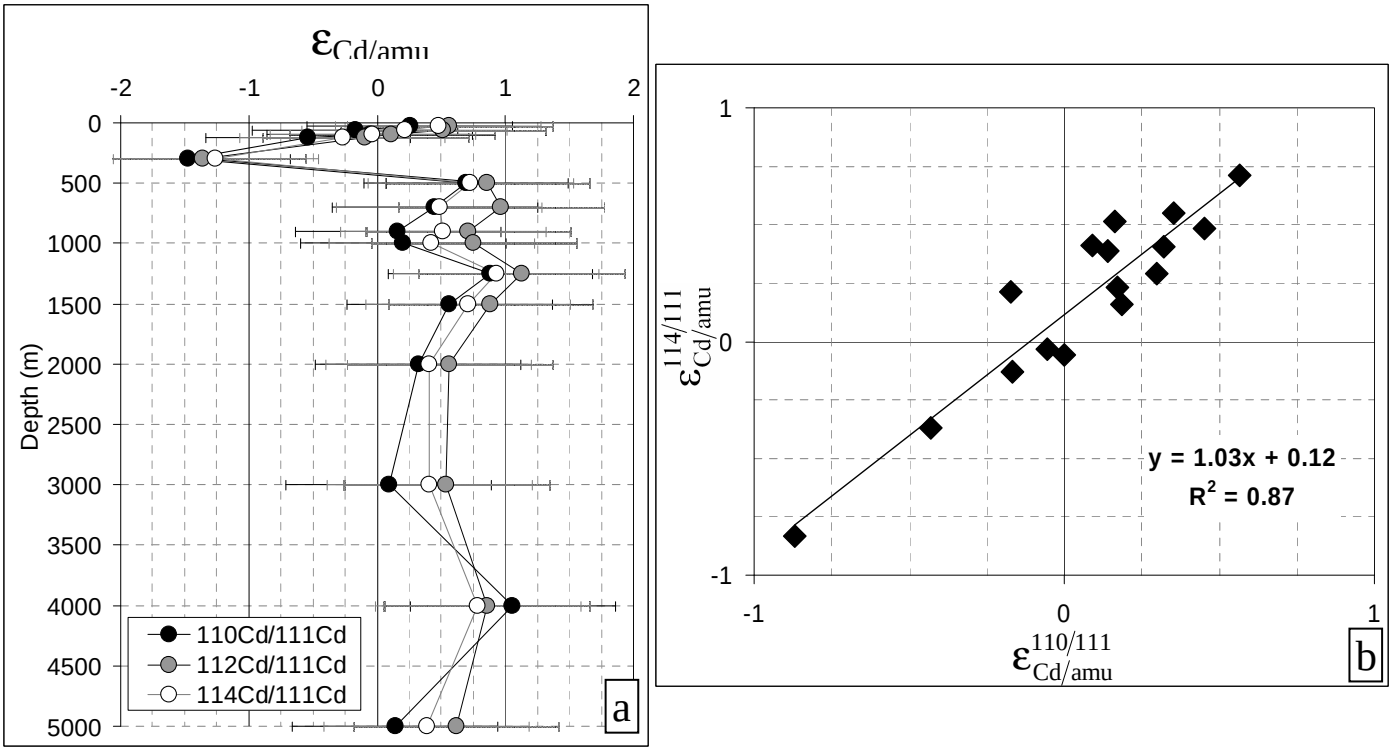
ε Cd/amu
-2
-1
0
1
2
Depth (m)
0
500
1000
1500
2000
2500
3000
3500
4000
4500
5000
110Cd/111Cd
112Cd/111Cd
114Cd/111Cd
a
1
0
-1
ε 114/111 Cd/amu
y = 1.03x + 0.12
R2 = 0.87
ε 110/111 Cd/amu
b

Figure 7

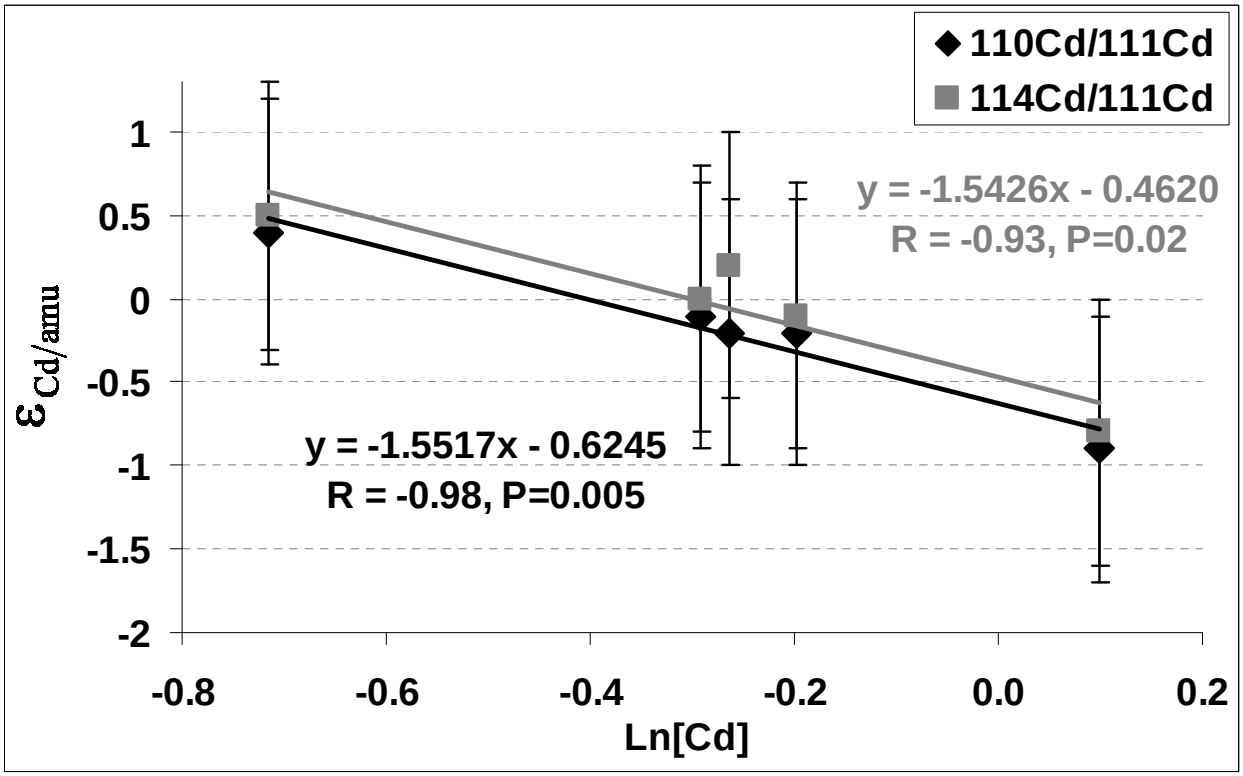
110Cd/111Cd
114Cd/111Cd
y = -1.5426x - 0.4620
R = -0.93, P=0.02
y = -1.5517x - 0.6245
R = -0.98, P=0.005
ε Cd/amu
Ln[Cd]
1
0.5
0
-0.5
-1
-1.5
-2
-0.8
-0.6
-0.4
-0.2
0.0
0.2

Figure 8

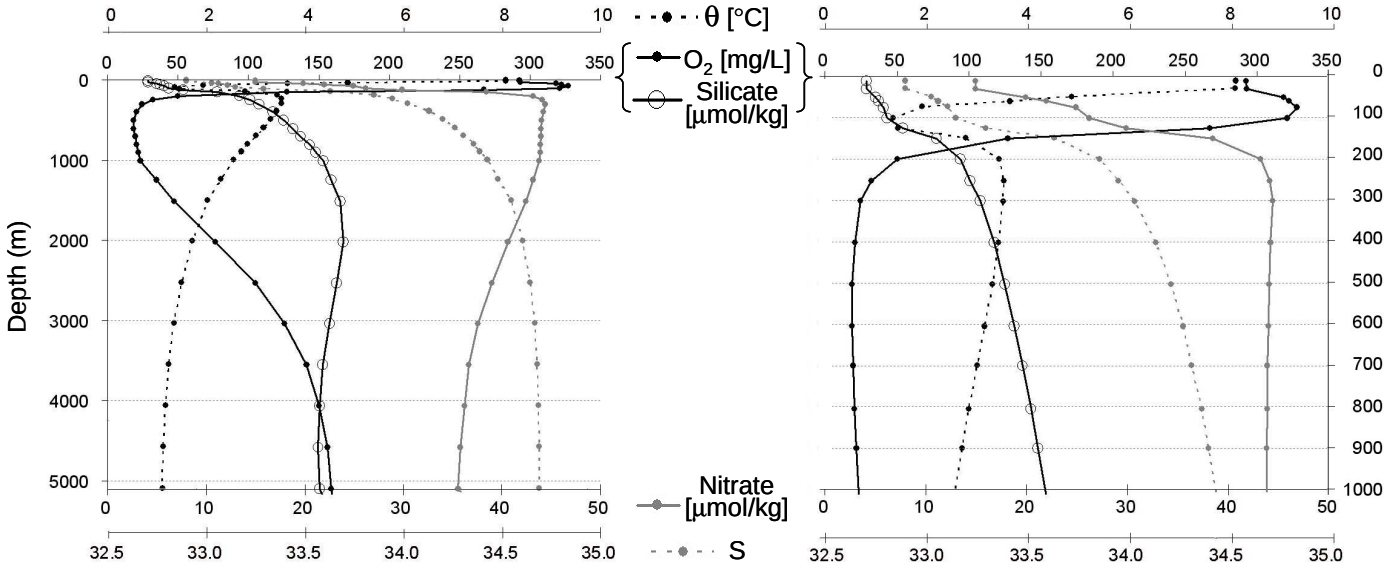

Figure 9

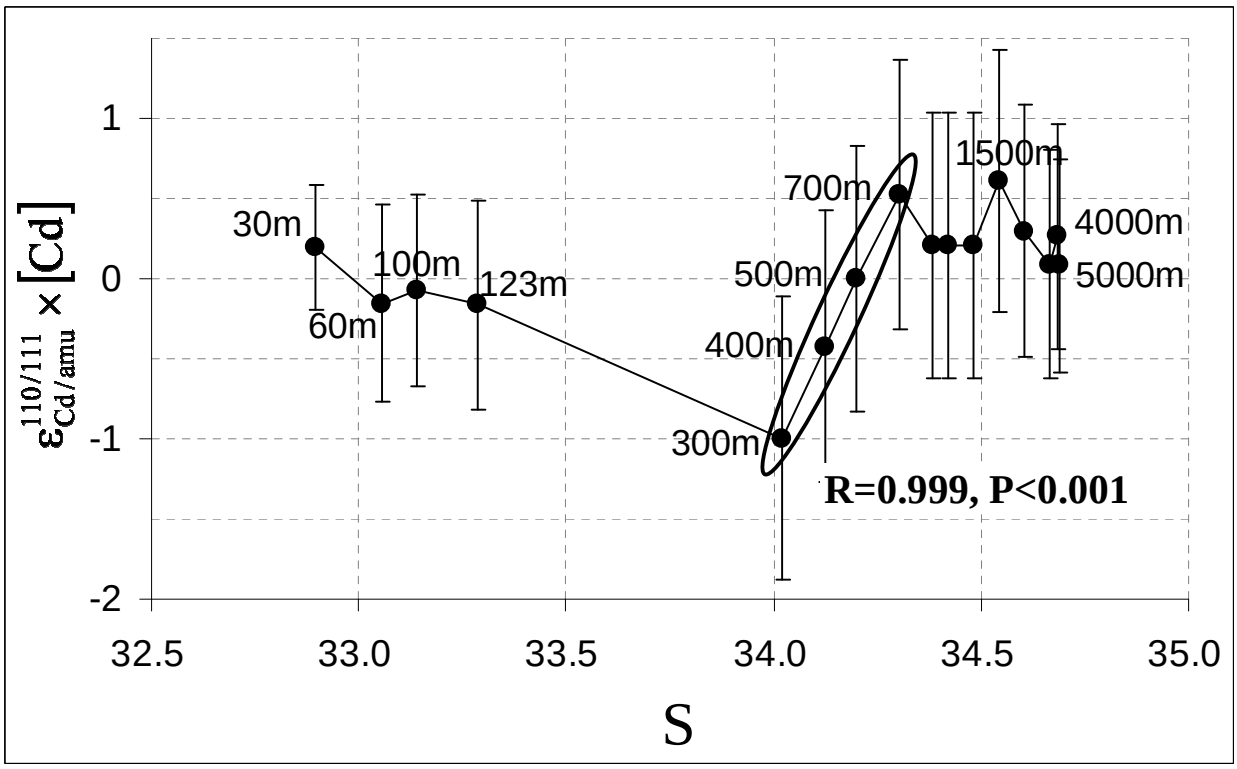
1
0
-1
-2
32.5
33.0
33.5
34.0
34.5
35.0
S
$\varepsilon^{110/111}_{Cd/amu} \times [Cd]$
30m
60m
100m
123m
300m
400m
500m
700m
1500m
4000m
5000m
R=0.999, P<0.001

Figure 10

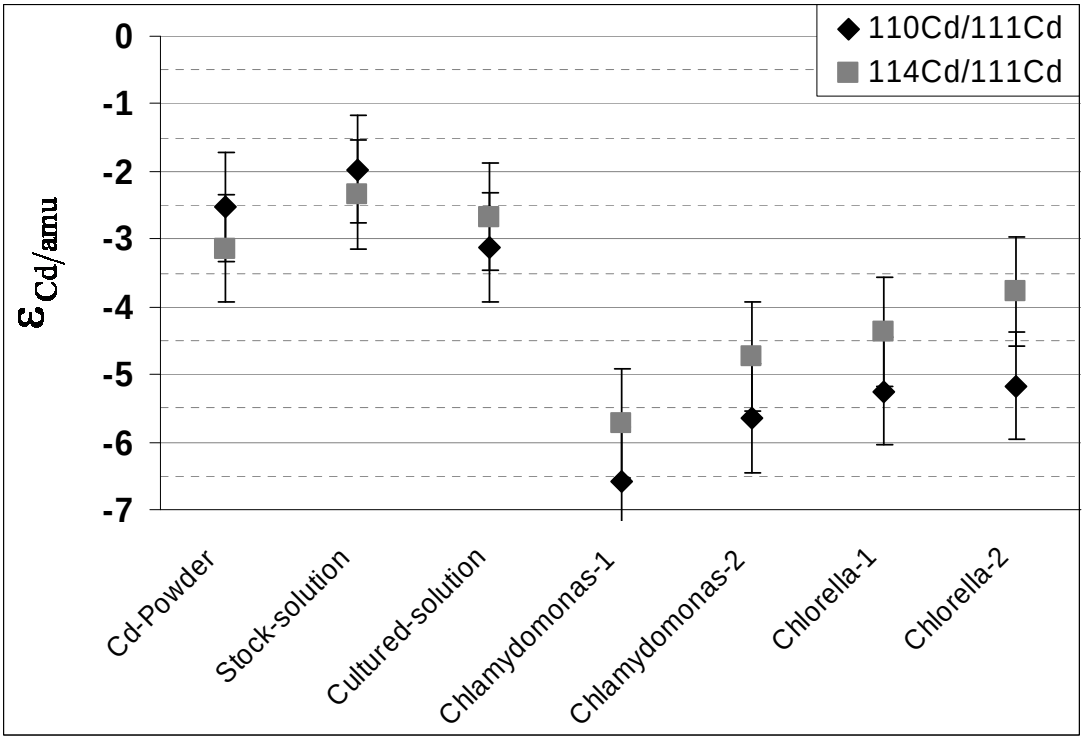
110Cd/111Cd
114Cd/111Cd
0
-1
-2
-3
-4
-5
-6
-7
ε Cd/amu
Cd-Powder
Stock-solution
Cultured-solution
Chlamydomonas-1
Chlamydomonas-2
Chlorella-1
Chlorella-2

Figure 11